

we evaluated wettability of CLPE-g-MPC cup by the spray method, because this method can be used non-destructively on large areas.

Since CLPE-g-MPC reduces the production of wear particles and bone-resorptive responses, periprosthetic osteolysis could be eliminated [12]. Based on the mechanical, tribological and biological advantages, we confidently expect CLPE-g-MPC be used in the next-generation of artificial hip joint systems.

## Conclusions

In this study, effects of a photo-induced radical graft polymerization technique on physical, mechanical and tribological properties of CLPE-g-MPC were investigated. The crystalline structure, physical and mechanical properties of the CLPE substrate were unchanged after the addition of a layer of MPC polymer by photo-polymerization. However, CLPE-g-MPC cups reduced 88% in the friction coefficient compared with untreated CLPE cups. After  $3.0 \times 10^6$  cycles in the hip joint simulator test, the wear rate of CLPE-g-MPC cups remained low. We concluded that the advantage of this photo-induced radical graft polymerization technique was that the grafted MPC polymer layer produces high lubricity while only affecting the surface, and has no effect on the properties of the CLPE substrate.

**Acknowledgements** This work was supported by a Grant-in-Aid for Scientific Research from the Japanese Ministry of Education, Culture, Sports, Science and Technology (#15390449), and a Health and Welfare Research Grant for Translational Research from the Japanese Ministry of Health, Labour and Welfare. The authors also express special thank to Dr. Fumiaki Miyaji, Mr. Yoshiki Ando and Mr. Takatoshi Miyashita (Japan Medical Materials Corp., Japan) for their excellent technical assistance.

## References

1. W. H. HARRIS, *Clin. Orthop.* **311** (1995) 46
2. A. KOBAYASHI, M. A. FREEMAN, W. BINEFIELD, Y. KADOYA, T. YAMAC, N. AL-SAFFER, G. SCOTT and P. A. REVELL, *J. Bone Joint Surg.* **79**(5) (1997) 844
3. D. H. SOCHART, *Clin. Orthop.* **363** (1999) 135
4. O. K. MURATOGLU, A. MARK, D. A. VITTETOE, W. H. HARRIS and H. E. RUBASH, *J. Bone Joint Surg.* **85A** (2003) 7
5. H. MCKELLOP, F. W. SHEN, B. LU, P. CAMPBELL and R. SALOVEY, *J. Orthop. Res.* **17**(2) (1999) 157
6. O. K. MURATOGLU, C. R. BRAGDON, D. O. O'CONNOR, M. JASTY and W. H. HARRIS, *J. Arthroplasty* **16** (2001) 149
7. D. W. MANNING, P. P. CHIANG, J. M. MARTELL, J. O. GALANTE and W. H. HARRIS, *Orthop. Res. Soc.* (2004) 1478
8. G. DIGAS, J. KÄRRHOLM, J. THANNER, H. MALCHAU and P. HERBERTS, *Clin. Orthop. Relat. Res.* **417** (2003) 126
9. C. HEICEL, M. SILVA, M. A. DELA ROSA and T. P. SCHMALZRIED, *J. Bone Joint Surg. Am.* **86**(4) (2004) 748
10. J. M. MARTELL, J. J. VERNER and S. J. INCAVO, *J. Arthroplasty* **18**(7) (2003) 55
11. H. OONISHI, S. C. KIM, Y. TAKAO, M. KYOMOTO, M. IWAMOTO and M. UENO, *J. Arthroplasty* **21**(7) (2006) 944
12. T. MORO, Y. TAKATORI, K. ISHIHARA, T. KONNO, Y. TAKIGAWA, T. MATSUSHITA, U. I. CHUNG, K. NAKAMURA and H. KAWAGUCHI, *Nature Mater.* **3** (2004) 829
13. K. ISHIHARA, R. ARAGAKI, T. UEDA, A. WATANABE and N. NAKABAYASHI, *J. Biomed. Mater. Res.* **24** (1990) 1069
14. K. ISHIHARA, N. P. ZIATS, B. P. TIERNEY, N. NAKABAYASHI and J. M. ANDERSON, *J. Biomed. Mater. Res.* **25**(11) (1991) 1397
15. K. J. KUIPER and J. E. NORDREHAUG, *Am. J. Cardiol.* **85** (2000) 698
16. M. GALLI, L. SOMMARIVA, F. PRATI, S. ZERBONI, A. POLITI, R. BONATTU, S. MAMELI, E. BUTTI, A. PAGANO and G. FERRARI, *Cathet. Cardiovasc. Intervent.* **53** (2001) 182
17. A. L. LEWIS, L. A. TOLHURST and P. W. STRATFORD, *Biomaterials* **23** (2002) 1697
18. K. ISHIHARA, Y. IWASAKI, S. EBIHARA, Y. SHINDO and N. NAKABAYASHI, *Colloids Surf. B, Biointerfaces* **18** (2000) 325
19. K. ISHIHARA, T. UEDA and N. NAKABAYASHI, *Polym. J.* **22**(5) (1990) 355
20. Swedish Transmission Research Institute, "Hydrophobicity Classification Guide", Guide 1, 92/1 (1992)
21. F. W. SHEN, H. A. MCKELLOP and R. SALOVEY, *J. Polym. Sci. Part B, Polym. Phys.* **34** (1996) 1063
22. M. H. NAKA, Y. MORITA and K. IKEUCHI, *Proc. Inst. Mech. Eng. [H]* **219**(3) (2005) 175
23. U. RAVIV, J. FREY, R. SAK, P. LAURAT, R. TADMOR and J. KLEIN, *Langmuir* **18** (2002) 7482
24. S. P. HO, N. NAKABAYASHI, Y. IWASAKI, T. BOLAND and M. LABERGE, *Biomaterials* **24** (2003) 5121
25. K. ISHIHARA, D. NISHIUCHI, J. WATANABE and Y. IWASAKI, *Biomaterials* **25** (2004) 1115
26. O. K. MURATOGLU, C. R. BRAGDON, D. O. O'CONNOR, M. JASTY, W. H. HARRIS, R. GUL and F. MCGARRY, *Biomaterials* **20** (1999) 1463

# Enhanced wear resistance of modified cross-linked polyethylene by grafting with poly(2-methacryloyloxyethyl phosphorylcholine)

Masayuki Kyomoto,<sup>1</sup> Toru Moro,<sup>2</sup> Tomohiro Konno,<sup>3</sup> Hiroaki Takadama,<sup>4</sup> Noboru Yamawaki,<sup>1</sup> Hiroshi Kawaguchi,<sup>2</sup> Yoshio Takatori,<sup>2</sup> Kozo Nakamura,<sup>2</sup> Kazuhiko Ishihara<sup>3</sup>

<sup>1</sup>Research and Development Corporate Division, Japan Medical Materials Corporation, Osaka, Japan

<sup>2</sup>Department of Orthopaedic Surgery, School of Medicine, The University of Tokyo, Tokyo, Japan

<sup>3</sup>Department of Materials Engineering, School of Engineering and Center for NanoBio Integration, The University of Tokyo, Tokyo, Japan

<sup>4</sup>Materials Research and Development Laboratory, Japan Fine Ceramics Center, Nagoya, Japan

Received 17 May 2006; revised 28 September 2006; accepted 28 September 2006

Published online 30 January 2007 in Wiley InterScience (www.interscience.wiley.com). DOI: 10.1002/jbm.a.31134

**Abstract:** We developed a cross-linked polyethylene (CLPE) modified with a phospholipid polymer in order to address the serious problem of osteolysis caused by wear particles derived from the polyethylene components of artificial hip joints. Our goal of preventing aseptic loosening could be achieved by avoiding any formation of CLPE wear particles or suppressing the activation of cell systems by the wear particles. We investigated the surface and wear resistance properties of 2-methacryloyloxyethyl phosphorylcholine (MPC) polymer grafted onto the surface of CLPE (CLPE-g-MPC). The relative density of MPC polymer chains was determined by the P–O group index. Generally, polymerization times correspond to the number of polymer chains in radical polymerization. After  $3.0 \times 10^6$

cycles in a hip joint simulator test, the steady wear rates of the untreated CLPE and CLPE-g-MPC cups with a low P–O group index were as high as  $4 \text{ mg}/10^6$  cycles; those of the CLPE-g-MPC cups with high P–O group indexes, that is, 0.46 and 0.48, markedly decreased to  $-1.12$  and  $0.16 \text{ mg}/10^6$  cycles, respectively. Therefore, the grafting of an MPC polymer with high density would be essential in order to maintain the long-term wear resistance of CLPE-g-MPC as an orthopedic bearing material. © 2007 Wiley Periodicals, Inc. *J Biomed Mater Res* 82A: 10–17, 2007

**Key words:** joint replacements; polyethylene; phospholipid; phosphorylcholine; wear mechanisms

## INTRODUCTION

As the number of aged persons in the world increases year by year, the increase in patients with poorly functioning joints due to external injury or disease is becoming a serious social problem. This means that the quality of artificial joints is becoming increasingly important. Most patients who receive an artificial joint experience a dramatic relief of pain

and enjoy a rapid improvement in the quality of life. The most widely used bearing couple for artificial joint systems is the combination of an ultra-high molecular weight polyethylene (UHMWPE) acetabular component and a metal (generally Co-Cr-Mo alloy) femoral component. However, osteolysis caused by wear particles of the UHMWPE is a serious problem with artificial hip joints.<sup>1–3</sup> Reducing wear particle production from UHMWPE is one way of preventing osteolysis. Efforts to decrease these particles have focused on using combinations other than metal-on-UHMWPE and improving the bearing materials themselves.

Several highly cross-linked polyethylenes (CLPE), irradiated with 50–105 kGy, have been launched since 1998 and used extensively.<sup>4,5</sup> Gamma and electron beam irradiation at various doses are used to produce CLPE and numerous *in vitro* studies have been performed using it. In published studies, CLPE subjected to 50–105 kGy exhibited an 80–90% reduc-

Correspondence to: M. Kyomoto, Japan Medical Materials Corporation, Uemura Nissei Bldg. 9F 3-3-31 Miyahara, Yodogawa-Ku, Osaka 532-0003, Japan; e-mail: kyomotom@jmmc.jp

Contract grant sponsor: Japanese Ministry of Education, Culture, Sports, Science, and Technology; contract grant number: 15390449

Contract grant sponsor: Japanese Ministry of Health, Labor, and Welfare

tion in wear rate compared with conventional polyethylene.<sup>6,7</sup> Furthermore, clinical results have confirmed CLPE's effective wear-resistance. However, while the efficacy of the CLPE is evidenced by these reports, *in vivo* the reduction of wear is reported to be only 40–60%.<sup>8–12</sup> Therefore, further improvement of CLPE is desirable.

Recently, we have developed a new-concept artificial hip joint with 2-methacryloyloxyethyl phosphorylcholine (MPC) polymer grafted onto the surface of CLPE (CLPE-g-MPC); it has been designed to reduce wear and suppress bone resorption.<sup>13</sup> MPC, a methacrylate monomer with a phospholipid polar group in the side chain, is a novel biomaterial designed and developed by Ishihara et al. that mimics the neutral phospholipids of biomembranes.<sup>14</sup> Various polymers containing MPC units are already widely used as biomaterials.<sup>15,16</sup> The biomembrane-like surface is readily obtained by treating the substrate materials with MPC polymer. The artificial biomembrane surface thus formed exhibits excellent biocompatibility; it is hydrophilic and forms a thin film of free water under physiological conditions.<sup>17</sup> Several medical devices have already been developed utilizing MPC polymer. These devices have been subjected to clinical use with the approval of the Food and Drug Administration of the USA; therefore, the efficacy and safety of the MPC polymer as a biomaterial are well established.<sup>18–20</sup>

We have been developing novel artificial joints with very-low-friction bearing surfaces by combining the biocompatible and hydrophilic MPC polymer with CLPE; this has been accomplished by using a photo-induced radical polymerization technique. This technique facilitates direct grafting of MPC to CLPE, thereby forming C—C covalent bonding between the MPC polymer and CLPE substrate. The advantage of this technique is that the MPC polymer graft occurs only on the CLPE surface and has no effect on the bulk properties of the CLPE substrate. The present study investigated the structure and properties of the MPC polymer layer formed on the CLPE surface by photo-induced radical graft polymerization. The wear-resistant properties of the CLPE-g-MPC are discussed in terms of the characteristics of the MPC polymer layer.

## MATERIALS AND METHODS

### Chemicals

Benzophenone and acetone were purchased from Wako Pure Chemical Industries (Osaka, Japan). 2-Methacryloyloxyethyl phosphorylcholine (MPC) was synthesized industrially using the method reported by Ishihara et al.<sup>14</sup> and was supplied by Ai Bio-Chips Co. (Tokyo, Japan).

### MPC graft polymerization

Compression-molded UHMWPE (GUR1020 resin; Poly Hi Solidur, IN) bar stock was  $\gamma$ -irradiated with 50 kGy in N<sub>2</sub> gas and annealed at 120°C for 7.5 h in N<sub>2</sub> gas for cross-linking. The cross-linked polyethylene (CLPE) specimens were machined from this bar stock after cooling. The specimens were immersed in an acetone solution containing 10 mg/mL benzophenone for 30 s and then dried in the dark to remove acetone at room temperature. The amount of benzophenone adsorbed on the surface was determined by ultraviolet spectroscopy to be  $3.5 \times 10^{-11}$  mol/cm<sup>2</sup> using a previously described method.<sup>21</sup> The MPC monomer was dissolved in degassed pure water to a concentration of 0.5 mol/L. The CLPE specimens coated with benzophenone were immersed in the aqueous MPC solution. The photo-induced graft polymerization on the CLPE surface was carried out with ultraviolet irradiation of 5 mW/cm<sup>2</sup> for 10–360 min at 60°C using a Toshiba D-35 filter that permitted the passage of ultraviolet light with a wavelength of  $350 \pm 50$  nm only. After the polymerization, the CLPE-g-MPC specimens were removed, washed with pure water and ethanol, and then dried. The CLPE-g-MPC specimens were gamma-sterilized with a dose of 25 kGy under N<sub>2</sub> gas.

### Surface analysis by using XPS, water-contact angle measurement, and FT-IR/ATR

The surface elemental conditions of the CLPE before and after MPC grafting were analyzed by X-ray photoelectron spectroscopy (XPS). The XPS spectra were obtained using an AXIS-HSi165 spectrophotometer (Kratos Analytical, UK) equipped with an Mg-K $\alpha$  radiation source at 15 kV at the anode. The take-off angle of the photoelectrons was maintained at 90°. Five scans were taken for each sample.

The static water-contact angle of the CLPE-g-MPC with various photo-polymerization periods was measured by a sessile drop method using an optical bench-type contact angle goniometer (Model DM300; Kyowa Interface Science Co., Saitama, Japan). Drops of purified water (1  $\mu$ L) were deposited onto the surface of the CLPE-g-MPC and the contact angles were directly measured with a microscope after each dropping (60 s), according to the ISO 15989 standard.<sup>22</sup> Fifteen replicate measurements were performed on each sample and the contact angle values were averaged.

The functional-group vibrations of the CLPE-g-MPC surface with various photo-polymerization periods were examined by Fourier-transform infrared (FT-IR) spectroscopy with attenuated total reflection (ATR) equipment. The measurements were performed over a range of 800–2000 cm<sup>-1</sup> by using an FT-IR analyzer (Perkin-Elmer FT-IR 1650; Perkin-Elmer Corp., MA) at a resolution of 4.0 cm<sup>-1</sup> for 100 scans.

The relative amount of grafted MPC polymer unit on the CLPE surface was evaluated by quantification of the phosphate (P—O) group that is contained within the structure of the MPC unit. The relative amount of phosphate

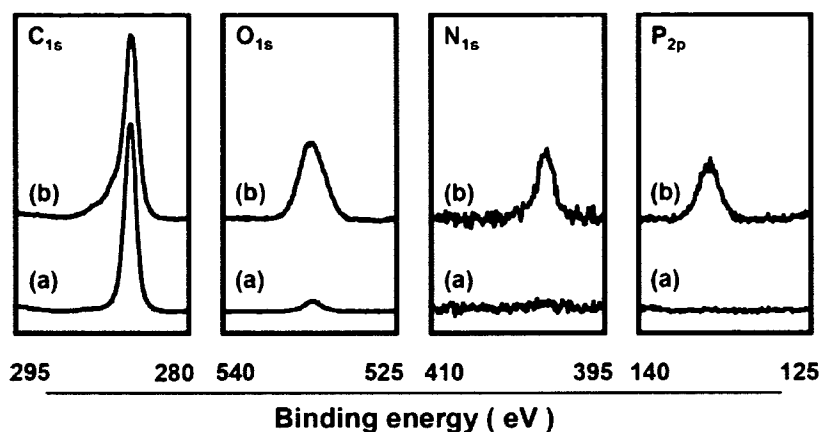


Figure 1. XPS spectra of CLPE-g-MPC. (a) CLPE (untreated), (b) CLPE-g-MPC.

group was defined as the P—O group index and was calculated as follows.

$$\text{P—O group index} = \frac{(1080 \text{ cm}^{-1} \text{ peak intensity})}{(1460 \text{ cm}^{-1} \text{ peak intensity})}$$

#### Cross-section of CLPE-g-MPC observed with TEM

A cross-section of the MPC polymer layer on the CLPE-g-MPC surface produced by various photo-polymerization periods was observed with a transmission electron microscope (TEM). The specimens (two pieces for each irradiation time) were first embedded in epoxy resin, stained with ruthenium oxide vapor at room temperature, and then sliced into ultra-thin films ( $\sim 100$ -nm thick) by using a Leica Ultra Cut UC microtome (Leica Microsystems, Wetzlar, Germany). A JEM-1010 electron microscope (JEOL, Tokyo, Japan) was used for the TEM observation at an acceleration voltage of 100 kV.

#### Hip simulation wear test

The inner and outer diameters of the CLPE-g-MPC cups used in the hip joint simulator were 26 mm and 52 mm, respectively. For each irradiation time (0, 23, 45, 90, and 180 min) four pieces were prepared. The wear test was performed using a 12-station hip joint simulator (MTS system Corp., MN). A 26-mm Co-Cr-Mo alloy femoral ball component (Japan Medical Materials Corp., Osaka, Japan) was used as an acetabular component. A mixture of 25% bovine serum, 20 mM/L of ethylenediaminetetraacetic acid (EDTA), and 0.1% sodium azide was used as lubricant, according to the ISO 14242-1 standard.<sup>23</sup> The lubricant was replaced every  $0.5 \times 10^6$  cycles. Walks, simulating a physiologic loading curve (Paul-type) with double peaks of 1793 and 2744N (183 and 280 kgf) loads, were applied with multidirectional (biaxial and orbital) motion of 1 Hz frequency. The wear was determined by weighing the polyethylene cups. Load-soak controls ( $n = 2$ ) were used to compensate for fluid absorption by the wear specimens.<sup>24</sup> The weights of the cups were measured every  $0.5 \times 10^6$

cycles. The testing continued until a total of  $3.5 \times 10^6$  cycles were completed.

To evaluate the net wear, corrected for any influence from plastic deformation, a melt-recovery operation was performed on selected samples of both CLPE and CLPE-g-MPC cups after the simulator tests, according to the method of Muratoglu et al.<sup>25</sup> The cups were melted at 150°C in a vacuum and allowed to cool down to the room temperature. The surface features of the bearing surfaces of the cups were observed with a confocal laser scanning microscope (OLS1200; Olympus Corp., Tokyo, Japan).

## RESULTS

Figure 1 shows the XPS spectra ( $C_{1s}$ ,  $O_{1s}$ ,  $N_{1s}$ , and  $P_{2p}$ ) of CLPE and CLPE-g-MPC. In the  $C_{1s}$  spectra of both CLPE and CLPE-g-MPC a strong peak was observed at 285 eV. This peak is attributed to the carbon atoms in the C—C or C—H groups. In the  $O_{1s}$  spectrum of CLPE-g-MPC, a significant peak assigned to the C—O group was observed at 532 eV. This peak is mainly ascribed to the MPC units. Even untreated CLPE exhibited a small peak at 532 eV. In this case, the peak is attributed to oxygen atoms and might suggest the contamination and/or oxidation of the CLPE surface. In the  $N_{1s}$  and  $P_{2p}$  spectra, clear peaks were observed for CLPE-g-MPC only. Peaks at 403 and 134 eV were assigned to the  $-N^+(\text{CH}_3)_3$  and phosphate groups, respectively; these peaks are characteristic of the phosphorylcholine in the MPC units. Table I summarizes the elemental compositions of the surfaces of untreated CLPE and CLPE-g-MPC. The measured contents of nitrogen (N) and phosphorous (P) in the CLPE-g-MPC was 5.1 and 5.2, respectively. These values were almost equivalent to the theoretical values ( $N = 5.3$ ,  $P = 5.3$ ) of MPC polymer.

Figure 2 shows the FT-IR/ATR spectra of CLPE and CLPE-g-MPC. A transmittance absorption peak was observed at  $1460 \text{ cm}^{-1}$  for both CLPE and

**TABLE I**  
Surface Elemental Compositions (%) of CLPE (Untreated) and CLPE-g-MPC

Samples	C	O	N	P
Untreated CLPE	99.6 (100.0)	0.4 (0.0)	0.0 (0.0)	0.0 (0.0)
CLPE-g-MPC	61.8 (57.9)	27.9 (31.6)	5.1 (5.3)	5.2 (5.3)

Theoretical elemental compositions of CLPE and MPC polymer are shown in the parentheses, respectively.

CLPE-g-MPC. This peak is attributed mainly to the methylene (CH<sub>2</sub>) chain in the CLPE substrate since the peak intensity is very strong and it is unchanged between the CLPE and the CLPE-g-MPC. However, the transmittance absorption peaks at 1240, 1080, and 970 cm<sup>-1</sup> were observed only for the CLPE-g-MPC. These peaks are ascribed to the phosphate (P—O) group in the MPC unit. Similarly, the transmittance absorption peak at 1720 cm<sup>-1</sup> observed for CLPE-g-MPC only corresponds to the ketone group in the MPC unit.

The relative P—O group index was calculated from the ratio of the FT-IR peak intensities at 1080 and 1460 cm<sup>-1</sup> as a measure of the amount of MPC unit grafted onto the CLPE surface; this was done because the peak intensity at 1460 cm<sup>-1</sup> remains unchanged.

Figure 3 shows the calculated P—O group index as a function of the irradiation time for the CLPE-g-MPC specimens. The P—O group index increased as the irradiation time was increased.

Figure 4 shows the static water-contact angle as a function of the calculated P—O group index for the CLPE-g-MPC specimens. The static water-contact

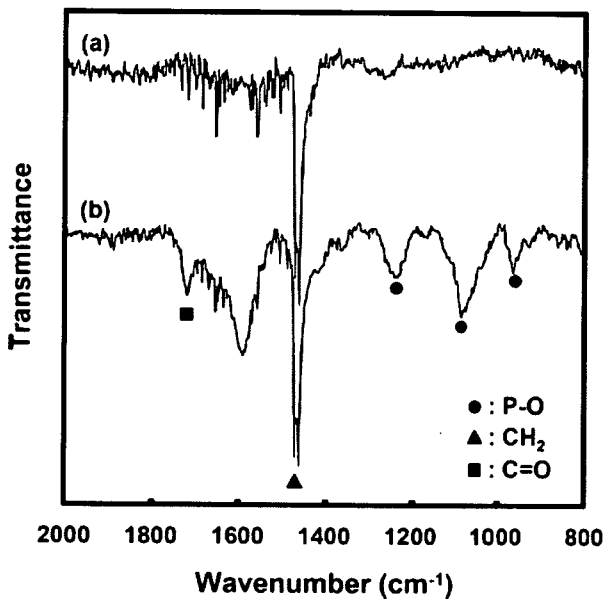


Figure 2. FT-IR/ATR spectra of CLPE-g-MPC. (a) CLPE (untreated), (b) CLPE-g-MPC.

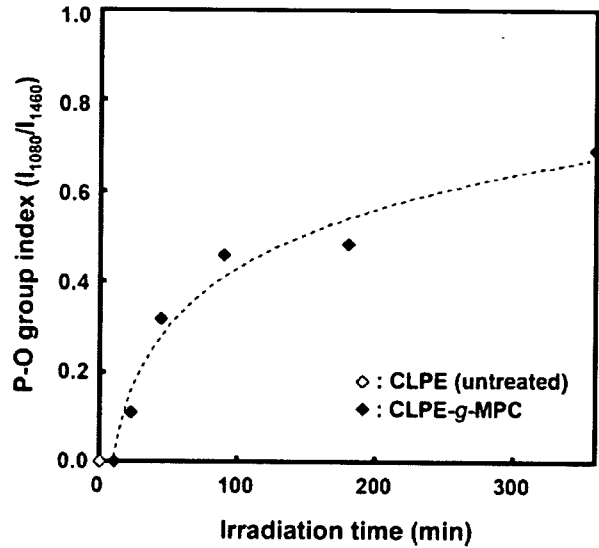


Figure 3. P—O group index as a function of irradiation time for CLPE-g-MPC.

angle on the untreated CLPE was 88° and decreased markedly with an increase in the P—O group index. When the P—O group index was greater than 0.3, the static water-contact angle became constant at the low value of 15°.

Figure 5 shows cross-sectional TEM images of CLPE-g-MPC produced with various ultraviolet irradiation times during polymerization. Lamellae of the order of 100–400 nm in length and 10–20 nm in thickness were observed in the CLPE substrate regardless of irradiation time, and the lamellae were 50–100 nm in length and 5–15 nm in thickness near the surface. With irradiation times longer than

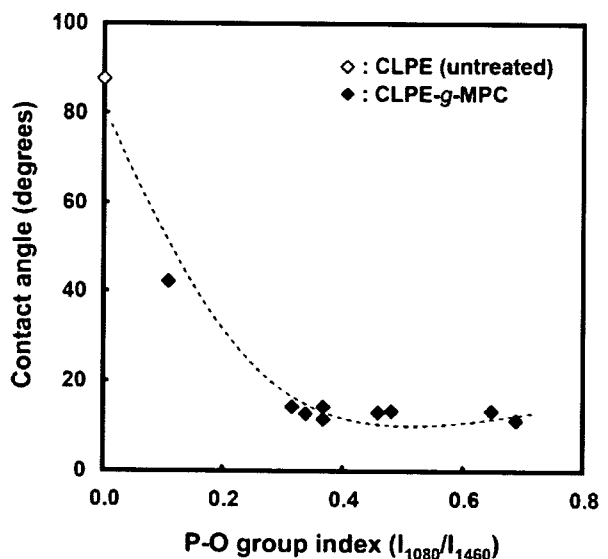


Figure 4. Static water-contact angle as a function of P—O group index for CLPE-g-MPC.

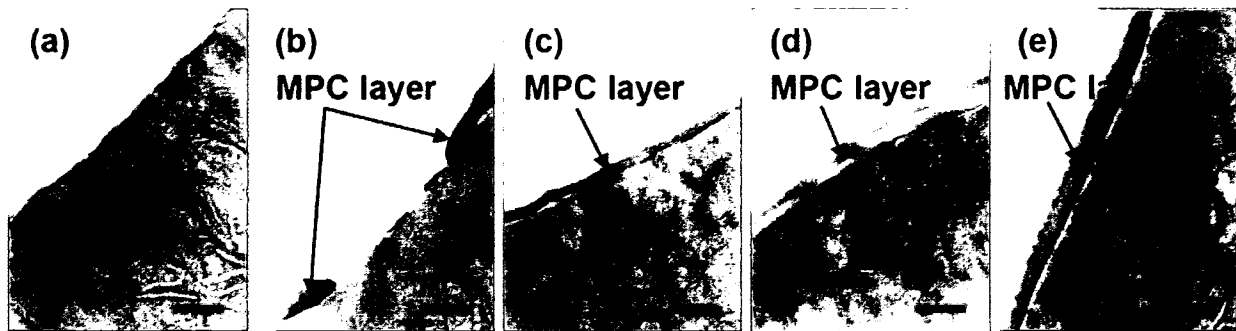


Figure 5. Cross-section TEM images of CLPE-g-MPC with various photo-polymerization times. Bar = 200 nm. (a) 11 min, (b) 23 min, (c) 45 min, (d) 90 min, and (e) 180 min.

45 min, a grafted MPC polymer layer 100–200 nm thick was clearly observed on the surface of the CLPE substrate. The MPC-covered region was coexistent with uncovered regions after an irradiation time of 23 min, although the thickness on the MPC polymer layer of the covered region remained the same (100–200 nm). With irradiation for 11 min, no MPC graft layer was observed on the surface of the CLPE. These results indicate that the density of the grafted MPC polymer can be controlled by the polymerization time. This is attributable to the fact that the number of polymer chains produced in a radical polymerization reaction is generally correlated with the photo-irradiation time.

Figure 6 shows the gravimetric wear of CLPE-g-MPC with various polymerization irradiation times during the hip joint simulation test. The CLPE-g-MPC cups were found to wear significantly less than the untreated CLPE cups. The wear of the CLPE-g-MPC cups subjected to 23 min of irradiation started to increase after  $2.5 \times 10^6$  cycles. Table II shows the wear rate of the CLPE-g-MPC cups with various P—O group indexes and irradiation times during the hip joint simulation test. We defined the initial wear rate as that from the start to  $0.5 \times 10^6$  cycles, and considered the steady wear rate as that from  $2.5 \times 10^6$  to  $3.0 \times 10^6$  cycles. All of the untreated CLPE and CLPE-g-MPC cups showed low initial wear rates of  $-1.42$  to  $-3.74$  mg/ $10^6$  cycles. The steady wear rate of the untreated CLPE cups and the CLPE-g-MPC cups with a low P—O group index of 0.11 increased to 3.68 and 4.64 mg/ $10^6$  cycles, respectively. In contrast, the wear rates of the CLPE-g-MPC cups with high P—O group indexes, that is, 0.46 and 0.48, were markedly lower at  $-1.12$  and  $0.16$  mg/ $10^6$  cycles, respectively.

Figure 7 shows the confocal laser scanning microscopy images of the bearing surfaces of the untreated CLPE and CLPE-g-MPC (irradiation time = 90 min) cups before and after the melt-recovery test that was performed after the simulator test. Before melt-recovery test, scratches were seen in the bearing sur-

faces of the untreated CLPE and CLPE-g-MPC. After melt-recovery test, these scratches completely disappeared from the bearing surfaces. In addition, clear regular circular machining marks were observed on the surface of the CLPE-g-MPC, while no marks were observed on the untreated CLPE, indicating that the former was not significantly worn.

## DISCUSSION

We have developed an artificial hip joint that uses CLPE-g-MPC on the bearing surface; it has been designed to reduce wear and suppress bone resorption. Our previous study reported the effects of graft polymerization of MPC onto the CLPE surface.<sup>13</sup> The MPC grafting markedly decreased the friction and amount of wear. In the present study, we investigated the structure and properties of the MPC polymer layer formed on the CLPE surface by photo-induced

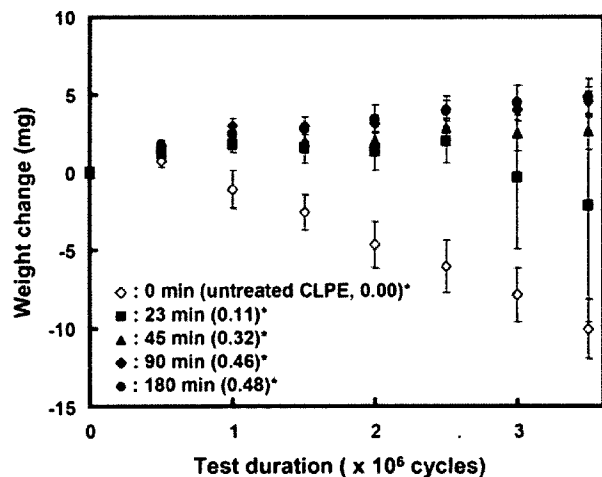


Figure 6. Weight change of CLPE-g-MPC cups with various irradiation times during polymerization in the hip joint simulation test. Bars = standard deviations. \*P—O group indexes are in parentheses.

**TABLE II**  
**Typical P—O Group Index and Wear Rate in Hip Joint Simulator Tests**

Irradiation Time (min)	P—O Group Index ( $I_{1080}/I_{1460}$ )	Initial Wear Rate (mg/ $10^6$ cycles)	Steady Wear Rate (mg/ $10^6$ cycles)
0 (untreated CLPE)	0.00	-1.42 (0.78)	3.68 (0.20)
23	0.11	-2.78 (0.76)	4.64 (6.38)
45	0.32	-2.58 (0.08)	0.68 (0.80)
90	0.46	-3.60 (0.48)	-1.12 (0.32)
180	0.48	-3.74 (0.50)	0.16 (0.08)

The standard deviation is in parentheses.

radical graft polymerization; this report discusses the wear-resistant properties of CLPE-g-MPC in terms of the characteristics of the MPC polymer layer.

After  $3.0 \times 10^6$  cycles of the hip joint simulator test, we confirmed that the CLPE-g-MPC cups with a P—O group index of 0.32 to 0.48 exhibited a relatively low steady wear rate (-1.12 to 0.68 mg/ $10^6$  cycles). This indicates that CLPE-g-MPC cups with a P—O group index greater than 0.32 achieve a >80% reduction in their steady wear rate compared with untreated CLPE as well as CLPE-g-MPC cups with a low P—O group index (0.11) and low density of grafted MPC polymer chains. Since MPC is a highly hydrophilic compound, poly(MPC) is water-soluble. In fact, as shown in Figure 4, the water-wettability of the CLPE-g-MPC surface was considerable greater than that of an untreated CLPE surface. Therefore, the artificial hip joint bearing with the grafted MPC

polymer surface exhibited considerably higher lubricity than that without the MPC polymer. The significant reduction in the coefficient of friction of the grafted MPC polymer<sup>13</sup> resulted in a substantial improvement in wear resistance. We assumed that the bearing surface of the artificial hip joint combined with MPC polymer exhibited the fluid film lubrication (or mixed lubrication) of the intermediate hydrated layer; this suggests that this novel artificial hip joint mimics the natural joint cartilage.

It is assumed that several important issues are involved in the long-term retention of the benefits of MPC polymer used in artificial joints under variable and multidirectional loads: strong bonding between the MPC polymer and the CLPE surface, high mobility of the free end groups of the MPC polymer, and a high density of the introduced MPC polymer. These considerations are based on previous studies

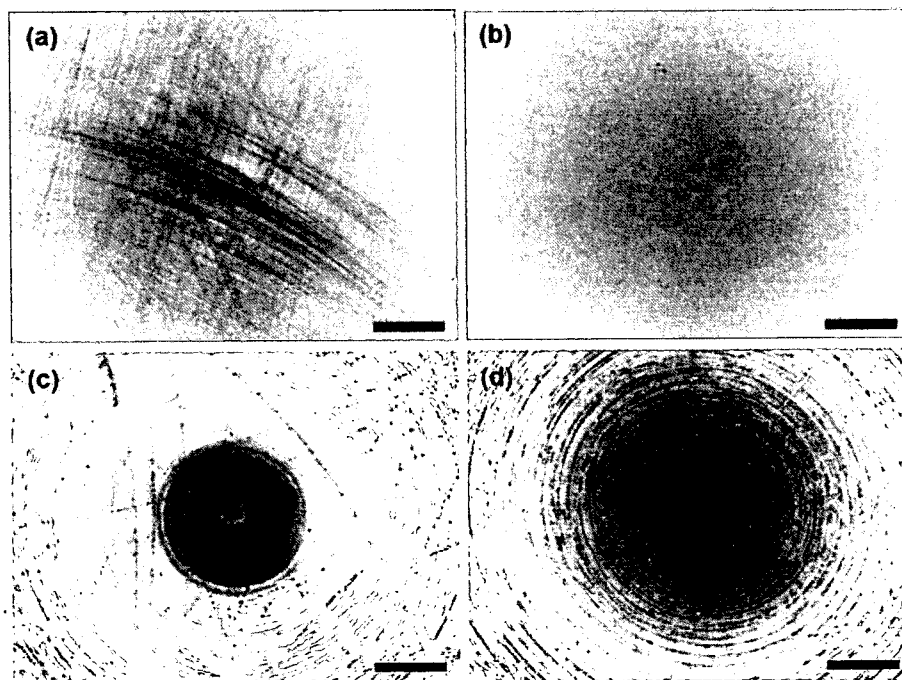


**Figure 7.** Confocal laser scanning microscope images of the bearing surfaces of the cups before and after a melt-recovery test that was performed after the simulator test. (a) CLPE before melt-recovery test, (b) CLPE after melt-recovery test, (c) CLPE-g-MPC before melt-recovery test, and (d) CLPE-g-MPC after melt-recovery test. Bar = 400  $\mu$ m.

of charged polymers (polyelectrolytes) reported by Raviv et al.<sup>26,27</sup> With this in mind, we selected photo-induced radical graft polymerization to produce C—C covalent bonding between a carbon atom of CLPE and an end group of the MPC polymer chain. As shown in Figure 5, the crystalline structure of the CLPE substrate is unchanged even after the grafting of MPC, regardless of irradiation time (polymerization time). This indicates that ultraviolet-induced radical graft polymerization does not affect the structure of the CLPE substrate. The unchanged structure of the CLPE substrate itself is very important because the CLPE cup acts not only as a bearing material but also as a structural material in the artificial hip joint. Furthermore, when the MPC layer disappears on the substrate surface, the exposed CLPE substrate may have lower wear than uncross-linked polyethylenes. We therefore deemed that the substrate was CLPE, although it was shielded by the MPC layer. In a previous study using gamma irradiation,<sup>28</sup> the lower-molecular-weight cross-linked GUR1020 materials had higher mechanical properties (tensile and impact properties) for all doses compared to the higher-molecular-weight cross-linked GUR1050 materials. Nevertheless, the cross-linked GUR1020 materials exhibited the same wear rate as the cross-linked GUR1050 materials. Therefore, we selected the GUR1020 compression-molded bar stock as a CLPE substrate.

To obtain an MPC polymer layer with high density, the irradiation time must be controlled.<sup>20</sup> The density of the MPC polymer chains on the surface of the CLPE gradually increased with increasing irradiation time and the entire surface of the CLPE was coated using polymerization times longer than 45 min. As shown in Figure 5, with longer irradiation, the thickness of the MPC polymer layer remained the same (100–200 nm). In the CLPE-g-MPC cups with a high surface density of MPC graft chains, the MPC graft chains are assumed to stand up to exhibit a brush like structure.<sup>29,30</sup> It is generally well-known that the reaction rate of radical polymerization is extremely high.<sup>31</sup> The molecular weight of grafted polymer is therefore controlled by monomer concentration. When the MPC polymer layer has brush like structure, the layer thickness might depend on the molecular weight of grafted MPC polymer. On the other hand, Figure 4 implies that the density of the MPC polymer chains on the surface of the CLPE was different, even if the water-wettability of the CLPE-g-MPC was constant (as low as 15°); this is because the P—O group index changed remarkably within the range of 0.3 and 0.7.

As mentioned above, the steady wear rate of CLPE-g-MPC cups with a high P—O group index was relatively low even after  $3.5 \times 10^6$  cycles in the simulator test. As shown in Figure 7, clear machining

marks with regular circles remained on the surface of CLPE-g-MPC cups even after the simulator test. In other words, the CLPE-g-MPC cups were virtually unworn, which is consistent with the relatively low wear observed in the hip joint simulator tests.

Table II shows that several CLPE-g-MPC cups exhibited a slight increase in weight (wear rate was negative); this was attributable to slightly enhanced fluid absorption over and above the fluid absorption by the load-soak controls. When using the gravimetric method, we corrected the weight loss for the fluid absorption by subtracting the weight gain that occurred in the load-soak controls. Since the wear cups are subjected to motion and load, there are limitations to this correction; therefore, they are observed to absorb slightly more fluid than their load-soak controls. However, as a result, the correction for fluid absorption by using the load-soak controls data as the correction factor leads to a slight underestimation of the actual weight loss.

The excellent functions of CLPE-g-MPC could avoid the activation of cell systems by the wear particles, thus entirely preventing periprosthetic osteolysis and subsequent aseptic loosening.<sup>13</sup> In view of its superior mechanical and biological advantages, the CLPE-g-MPC is widely expected to be the next-generation bearing material for artificial hip joints. Arrangements are now being made for the conduction of clinical trials.

In this study, we investigated the surface physical properties of CLPE-g-MPC. After a hip joint simulator test, we confirmed that CLPE-g-MPC cups with a high surface density of MPC graft chains exhibited a relatively low and steady wear rate. When compared with cups with untreated CLPE and those with CLPE-g-MPC with a low P—O group index (cups with low density of grafted MPC polymer chain), these CLPE-g-MPC cups exhibited an 80% reduction in their steady wear rate. Thus, it appears that CLPE-g-MPC markedly reduces the generation of wear particles. However, the grafting of MPC polymer at a high density is essential to maintain the wear-resistance of CLPE-g-MPC as an orthopedic bearing material over long periods of time. We conclude that grafting MPC onto CLPE is a useful method for maintaining efficient lubrication of artificial hip joints over a long period.

The authors thank Dr. Fumiaki Miyaji, Mr. Yoshiki Ando, and Mr. Takatoshi Miyashita (Japan Medical Materials Corp., Osaka, Japan) for their excellent technical assistance.

## References

1. Harris WH. The problem is osteolysis. *Clin Orthop* 1995;311:46–53.



2. Kobayashi A, Freeman MA, Bonfield W, Kadoya Y, Yamac T, Al-Saffar N, Scott G, Revell PA. Number of polyethylene particles and osteolysis in total joint replacements. A quantitative study using a tissue-digestion method. *J Bone Joint Surg Br* 1997; 79:844–848.
3. Sochart DH. Relationship of acetabular wear to osteolysis and loosening in total hip arthroplasty. *Clin Orthop* 1999;363: 135–150.
4. Collier JP, Currier BH, Kennedy FE, Currier JH, Timmins GS, Jackson SK, Brewer RL. Comparison of cross-linked polyethylene materials for orthopaedic applications. *Clin Orthop Relat Res* 2003;414:299–304.
5. Muratoglu OK, Mark A, Vittetoe DA, Harris WH, Rubash HE. Polyethylene damage in total knees and use of highly crosslinked polyethylene. *J Bone Joint Surg Am* 2003;85:S7–S13.
6. McKellop H, Shen FW, Lu B, Campbell P, Salovey R. Development of an extremely wear-resistant ultra high molecular weight polyethylene for total hip replacements. *J Orthop Res* 1999;17:157–167.
7. Muratoglu OK, Bragdon CR, O'Connor DO, Jasty M, Harris WH. A novel method of crosslinking ultra-high-molecular-weight polyethylene to improve wear, reduce oxidation, and retain mechanical properties. Recipient of the 1999 HAP Paul Award. *J Arthroplasty* 2001;16:149–160.
8. Manning DW, Chiang PP, Martell JM, Galante JO, Harris WH. In vivo comparative wear study of traditional and highly cross-linked polyethylene in total hip arthroplasty. *J Arthroplasty* 2005;20:880–886.
9. Digas G, Kärrholm J, Thanner J, Malchau H, Herberts P. Highly cross-linked polyethylene in cemented THA. *Clin Orthop Relat Res* 2003;417:126–138.
10. Heichel C, Silva M, dela Rosa MA, Schmalzried TP. Short-term in vivo wear of cross-linked polyethylene. *J Bone Joint Surg Am* 2004;86:748–751.
11. Martell JM, Verner JJ, Incavo SJ. Clinical performance of a highly cross-linked polyethylene at two years in total hip arthroplasty: A randomized prospective trial. *J Arthroplasty* 2003;18:55–59.
12. Oonishi H, Kim SC, Takao Y, Kyomoto M, Iwamoto M, Ueno M. Wear of highly cross-linked polyethylene acetabular cup in Japan. *J Arthroplasty* 2006;18:944–949.
13. Moro T, Takatori Y, Ishihara K, Konno T, Takigawa Y, Matsushita T, Chung UI, Nakamura K, Kawaguchi H. Surface grafting of artificial joints with a biocompatible polymer for preventing periprosthetic osteolysis. *Nat Mater* 2004;3:829–837.
14. Ishihara K, Ueda T, Nakabayashi N. Preparation of phospholipid polymers and their properties as polymer hydrogel membranes. *Polym J* 1990;22:355–360.
15. Ishihara K, Aragaki R, Ueda T, Watanabe A, Nakabayashi N. Reduced thrombogenicity of polymers having phospholipid polar groups. *J Biomed Mater Res* 1990;24:1069–1077.
16. Ishihara K, Ziats NP, Tierney BP, Nakabayashi N, Anderson JM. Protein adsorption from human plasma is reduced on phospholipids polymers. *J Biomed Mater Res* 1991;25:1397–1407.
17. Kitano H, Imai M, Mori T, Gemmei-Ide M, Yokoyama Y, Ishihara K. Structure of water in the vicinity of phospholipid analogue copolymers as studied by vibrational spectroscopy. *Langmuir* 2003;19:10260–10266.
18. Kuiper KJ, Nordrehaug JE. Early mobilization after protamine reversal of heparin following implantation of phosphorylcholine-coated stents in totally occluded coronary arteries. *Am J Cardiol* 2000;85:698–702.
19. Galli M, Sommariva L, Prati F, Zerboni S, Politi A, Bonatti R, Mameli S, Butti E, Pagano A, Ferrari G. Acute and mid-term results of phosphorylcholine-coated stents in primary coronary stenting for acute myocardial infarction. *Catheter Cardiovasc Interv* 2001;53:182–187.
20. Lewis AL, Tolhurst LA, Stratford PW. Analysis of a phosphorylcholine-based polymer coating on a coronary stent pre- and post-implantation. *Biomaterials* 2002;23:1697–1706.
21. Ishihara K, Iwasaki Y, Ebihara S, Shindo Y, Nakabayashi N. Photoinduced graft polymerization of 2-methacryloyloxyethyl phosphorylcholine on polyethylene membrane surface for obtaining blood cell adhesion resistance. *Colloids Surf B* 2000; 18:325–335.
22. ISO. Plastics—Film and sheeting—Measurement of water-contact angle of corona-treated films. 2004. International Organization for Standardization 15989.
23. ISO. Implants for surgery: Wear of total hip-joint prostheses, Part 1: Loading and displacement parameters for wear-testing machines and corresponding environmental conditions for test. 2002. International Organization for Standardization 14242-1.
24. ISO. Implants for surgery: Wear of total hip-joint prostheses, Part 2: Methods of measurement. 2000. International Organization for Standardization 14242-2.
25. Muratoglu OK, Greenbaum ES, Bragdon CR, Jasty M, Freiberg AA, Harris WH. Surface analysis of early retrieved acetabular polyethylene liners: A comparison of conventional and highly crosslinked polyethylenes. *J Arthroplasty* 2004;19: 68–77.
26. Raviv U, Frey J, Sak R, Laurat P, Tadmor R, Klein J. Properties and interactions of physigrafted end-functionalized poly (ethylene glycol) layers. *Langmuir* 2002;18:7482–7495.
27. Raviv U, Glasson S, Kampf N, Gohy JF, Jérôme R, Klein J. Lubrication by charged polymers. *Nature* 2003;425:163–165.
28. Greer KW, King RS, Chan FW. The effects of raw material, irradiation dose, and irradiation source on crosslinking of UHMWPE. In: Kurtz SM, Gsell RA, Martell J, editors. *Cross-linked and Thermally Treated Ultra-High Molecular Weight Polyethylene for Joint Replacements*. West Conshohocken: American Society for Testing and Materials; 2003. pp 209–220.
29. Matsuda T, Kaneko M, Ge S. Quasi-living surface graft polymerization with phosphorylcholine group(s) at the terminal end. *Biomaterials* 2003;24:4507–4515.
30. Goda T, Konno T, Takai M, Moro T, Ishihara K. Biomimetic phosphorylcholine polymer grafting from polydimethylsiloxane surface using photo-induced polymerization. *Biomaterials* 2006;27:5151–5160.
31. Feng W, Brash J, Zhu S. Atom-transfer radical grafting polymerization of 2-methacryloyloxyethyl phosphorylcholine from silicon wafer surface. *J Polym Sci Part A: Polym Chem* 2004;42: 2931–2942.

# Friction behavior of high-density poly(2-methacryloyloxyethyl phosphorylcholine) brush in aqueous media

Motoyasu Kobayashi,<sup>a</sup> Yuki Terayama,<sup>b</sup> Nao Hosaka,<sup>b</sup> Masataka Kaido,<sup>c</sup> Atsushi Suzuki,<sup>c</sup> Norifumi Yamada,<sup>d</sup> Naoya Torikai,<sup>d</sup> Kazuhiko Ishihara<sup>e</sup> and Atsushi Takahara<sup>\*ab</sup>

Received 31st October 2006, Accepted 13th March 2007

First published as an Advance Article on the web 28th March 2007

DOI: 10.1039/b615780g

Super-hydrophilic polymer brushes were prepared by surface-initiated atom transfer radical polymerization of 2-methacryloyloxyethyl phosphorylcholine (MPC) on initiator-immobilized silicon wafers. The graft density was estimated to be *ca.* 0.22 chains nm<sup>-2</sup> based on the linear relationship between  $M_n$  and the layer thickness. The contact angle against water was very low, and air bubbles in water hardly attached onto the brush surface, indicating a super-hydrophilic surface. Neutron reflectivity measurements of the poly(MPC) brush showed that the grafting polymer chains extended a fair amount in the vertical direction from the substrate in a good solvent such as water, while they shrank in a poor solvent. Frictional properties of the poly(MPC) brushes were characterized by sliding a glass ball probe in air and various solvents under a load of 0.49 N at a sliding velocity of 90 mm min<sup>-1</sup>. An extremely low friction coefficient of the poly(MPC) brush was observed in humid atmosphere because water molecules adsorbed into the brush layer acted as a lubricant.

## Introduction

Generally, water is not a suitable lubricant for bearing or engineering friction systems on the surface of inorganic materials because an effective boundary layer cannot be formed by water alone at the friction interface due to its low viscosity compared with lubrication oils. However, water lubrication systems are an environmental friendly technology, advantageous for heat management, and economical. Actually, living organisms have excellent biolubrication systems with extremely low friction in cartilage, the vitreous body of the eyes, and synovial joints, such as hip, knee and finger joints, supported by water-retention materials consisting of collagen tissue, hyaluronic acid hydrogel, and glycoprotein.<sup>1,2</sup> Recently, several artificial approaches have been employed to investigate boundary lubrication in aqueous media. Tethering long polymer chains on a flat surface with a sufficiently high surface density forms polymer brushes,<sup>3</sup> which are widely used for modification of substrates. Water-lubrication systems supported by hydrophilic polymer brushes have been extensively studied due to their unique tribological properties. Klein, who is one of the pioneers in tribology of polymer brushes, and his coworkers discovered the reduction

of frictional forces between solid surfaces bearing tethered polymers using a surface force balance, and they also reported that brushes of charged polymer (polyelectrolyte) could act as efficient lubricants between mica surfaces in an aqueous medium, even though the graft density was not so high.<sup>4-6</sup> Similarly, Osada *et al.* reported that gel-terminated polyelectrolyte brushes, prepared by controlled radical polymerization using 2,2,6,6-tetramethyl-1-piperidinyloxy (TEMPO) radicals, reduce the friction force between the hydrogels and a glass plate across water.<sup>7</sup> They also describe that longer polyelectrolyte molecules exhibited even higher friction than did a normal network gel. Sheth *et al.* measured the normal forces between poly(ethylene glycol) brushes against various surfaces.<sup>8</sup> They found that the brushes did not adhere to a neutral lipid bilayer or to bare mica. The lubrication properties of poly(L-lysine)-graft-poly(ethylene glycol) adsorbed on silicon oxide and iron oxide surfaces have been studied by Spencer and his coworkers using ultra-thin-film interferometry, mini traction machines and pin-on-disk tribometry.<sup>9,10</sup> They reported that the graft polymer forms a stable lubricant layer on the tribological interface in aqueous solution and reduces friction.

Over the last decades, high-density and well-defined polymer brushes have been readily synthesized owing to the progress in surface-initiated atom transfer radical polymerization (ATRP) techniques.<sup>11</sup> Tsujii and his collaborators have measured topographic images and force–distance profiles of high-density PMMA brushes by scanning force microscopy using a micro silica sphere attached to a cantilever head.<sup>12</sup> Under the high graft density, the osmotic pressure extends the grafted polymer chains in the vertical direction, which gives rise to extremely strong resistance against compression. The steric repulsion between the polymers supporting high normal loads gives low frictional forces between the brush-bearing surfaces. Extremely

<sup>a</sup>The Institute for Materials Chemistry and Engineering, Kyushu University, 744 Motoooka, Nishi-ku, Fukuoka 819-0395, JAPAN. E-mail: takahara@cstf.kyushu-u.ac.jp; Fax: +81-92-802-2518; Tel: +81-92-802-2517

<sup>b</sup>Graduate School of Engineering, Kyushu University, 744 Motoooka, Nishi-ku, Fukuoka 8129-0395, JAPAN

<sup>c</sup>TOYOTA Motor Co., 1 Toyota-cho, Toyota, Aichi 472-8572, JAPAN

<sup>d</sup>Neutron Science Laboratory, High Energy Accelerator Research Organization, 1-1 Oho, Tsukuba, Ibaraki 305-0801, JAPAN

<sup>e</sup>Department of Materials Engineering, Graduate School of Engineering, The University of Tokyo, 7-3-1 Hongo, Bunkyo-ku, Tokyo 110-8586, JAPAN

low friction coefficients were observed in nano-tribological studies performed by atomic force microscopy (AFM) using colloidal probes immobilized with high-density PMMA brushes in toluene.<sup>13</sup> Macroscopic friction testing of a high-density PMMA brush was also carried out using a stainless ball as a sliding probe, resulting in low-friction and a good wear-resistant surface under a high normal load.<sup>14</sup> The authors have also reported that hydrophilic polymer brushes with hydroxy groups on the side chains exhibited a low friction coefficient in water.<sup>15</sup> The present study focused on specially-designed methacrylate containing a phosphorylcholine unit in the side chain, 2-methacryloyloxyethyl phosphorylcholine (MPC), of which synthesis and polymerization were first reported in 1990.<sup>16</sup> Poly(MPC) is well known as a super-hydrophilic and biocompatible polymer,<sup>17</sup> therefore, control of protein adsorption and cell manipulations by well-defined poly(MPC) brush surfaces has attracted much attention.<sup>18,19</sup> Ho *et al.* observed significantly low frictional coefficients with a polyurethane catheter material surface coated with poly(MPC-*co-n*-butyl methacrylate) under wet conditions.<sup>20</sup> The application to medical implant devices such as artificial joints<sup>21</sup> has also been extended taking advantage of the low friction properties and biocompatibility of poly(MPC) brushes.

A large number of papers focusing on the preparation and characterization of polyelectrolyte brushes have been published<sup>22,23</sup> since the pioneering theoretical works started by Miklavic and Marčelja<sup>24</sup> in the 1980s. The effect of charge density, chain length, graft density,<sup>25–27</sup> ionic strength<sup>28</sup> and solvent quality<sup>29,30</sup> on the structure of polyelectrolyte brushes have been successively investigated precisely. Experimental studies have also been performed to measure the repulsive and attractive interactions of polyelectrolyte brushes,<sup>31,32</sup> because of the importance in understanding colloidal stability<sup>33</sup> and the electrostatic interactions between proteins and the charged brush.<sup>34</sup> Direct measurements of the forces acting between polyelectrolyte brushes were demonstrated by Kurihara *et al.*<sup>35</sup> Kelly *et al.* measured interactions between polyelectrolyte covered surfaces and Si<sub>3</sub>N<sub>4</sub> cantilevers in salt solution by AFM.<sup>36</sup> Lubrication properties of polyelectrolyte brushes have been investigated by Klein and his coworkers.<sup>4–6</sup> However, the great majority of polyelectrolyte brushes mentioned above is prepared by adsorption of comb-like polyelectrolyte on the solid surface, by grafting-to methods using an end-functionalized polymer, by grafting-from methods using classical free radical polymerization, and by LB methods using charged diblock copolymers at the air–water interface. Although the various types of well-defined polyelectrolyte brushes are synthesized by controlled polymerization systems nowadays, the frictional properties of polyelectrolyte brushes, especially high-density grafted polyelectrolytes, have not been investigated yet in detail, with some exceptions. This work is expected to contribute to the field of tribological study of well-defined polyelectrolyte brushes.

In this study, the authors investigate macroscopic tribology and mechanical properties of a poly(MPC) brush under a load of 10<sup>8</sup> Pa pressure from the viewpoint of practical engineering applications. Water lubrication systems supported by a high-density poly(MPC) brush are expected to afford a low friction surface.

## Experimental

### Materials

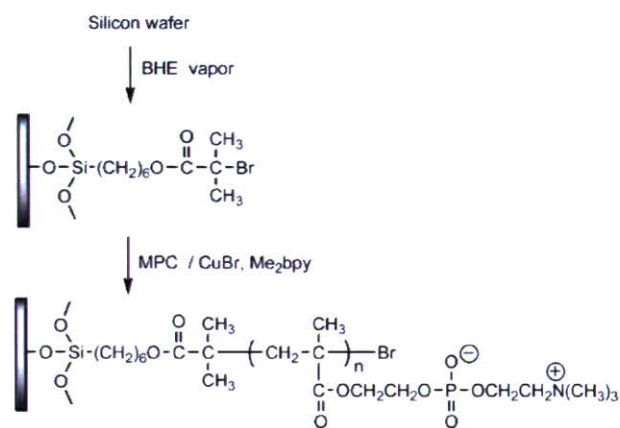
Methanol was purified by refluxing over magnesium for 6 h followed by distillation under ambient pressure. CuBr (Wako, 98%) was purified by washing with acetic acid and ethanol and was dried under vacuum. Ethyl 2-bromoisobutyrate (EB) (TCI, 99%) was used as received. 6-Triethoxysilylhexyl 2-bromoisobutyrate (BHE)<sup>37</sup> was synthesized by hydrosilylation of 5-hexenyl 2-bromoisobutyrate<sup>38</sup> treated with triethoxysilane using Karstedt catalyst. MPC monomer was prepared with the procedure reported in the previous paper.<sup>16</sup> Water for contact angle measurements and frictional tests was purified with the NanoPure Water system (Millipore, Inc.).

### Initiator-immobilized silicon substrate

The silicon (111) wafers (10 × 40 mm pieces) were cleaned by washing with piranha solution (H<sub>2</sub>SO<sub>4</sub>–H<sub>2</sub>O<sub>2</sub> = 7 : 3, v/v) at 373 K for 1 h and by exposure to vacuum ultraviolet-rays (VUV, λ = 172 nm) for 5 min under reduced pressure (30 Pa). These silicon wafers and a glass vessel filled with 10% toluene solution of BHE were packed in a glass container purged with N<sub>2</sub> gas, and were allowed to stand in a heating oven at 373 K for 5 h. During the heating at this temperature, BHE vapor adsorbed on the surface of the wafers to make an organosilane monolayer, which is known as the chemical vapor adsorption (CVA) method.<sup>39</sup> After these wafers were rinsed with toluene and ethanol, they were dried *in vacuo* at 373 K for 1 h and were stored in a dark place. The surface chemical composition was investigated with X-ray photoelectron spectroscopy (XPS).

### General procedure for surface-initiated ATRP of MPC

A typical surface-initiated ATRP of MPC was performed as follows (Scheme 1). A few sheets of the initiator-immobilized silicon wafers, CuBr (0.025 mmol), and 4,4'-dimethyl-2,2'-bipyridyl (0.050 mmol) were introduced into a glass tube with a stopcock and were dried by repeating a degas and argon purge. A methanol solution of MPC (6.5 mmol) and EB (0.0125 mmol) was added to the catalyst. Oxygen was removed by freeze-pump-thaw cycles. The polymerization reaction was conducted at 303 K for 12 h under argon to simultaneously



Scheme 1

generate poly(MPC) brush from the substrate and free poly(MPC) from EB. The reaction was stopped by opening the glass vessel to air, and the reaction mixture was poured into THF to precipitate the free polymer. The silicon wafers were washed with methanol using a Soxhlet apparatus for 12 h to remove the free polymer absorbed on their surfaces, and were dried under the reduced pressure at 373 K for 1 h. The free polymer in methanol solution was passed through a neutral alumina column to remove catalyst, and was poured into THF to precipitate the free polymer.

## Measurements

The number-average molecular weights ( $M_n$ ) and molecular weight distribution (MWD) of the free polymer were determined by size-exclusion chromatography (SEC) recorded on a JASCO instrument equipped with JASCO 2031plus RI detection, which runs through two directly connected poly-(hydroxyethyl methacrylate) gel columns (Shodex OHpak SB-804HQ,  $0.5 \text{ mL min}^{-1}$ ) using water containing 0.01 M LiBr as an eluent at 298 K. A calibration curve was made using a series of well-defined poly(MPC)s prepared by controlled polymerization based on the reversible fragmentation chain transfer (RAFT) system. The thickness of the polymer brush and the spin coat film on the silicon substrate were determined by an imaging ellipsometer (Nippon Laser & Electronics Lab.) equipped with a YAG laser (532.8 nm). The polarizer angle was fixed at  $50^\circ$ , and a refractive index of 1.48 was assumed for the calculations of the film thickness. AFM observation was done with SPA 400 with an SPI 3800N controller (SII NanoTechnology Inc.) in air at room temperature, using a  $\text{Si}_3\text{N}_4$  integrated tip on a commercial triangle  $200 \mu\text{m}$  cantilever (Olympus Co., Ltd.) with a spring constant of  $0.09 \text{ N m}^{-1}$ . The contact angles against water, hexadecane, and methylene iodide (each droplet volume was  $2 \mu\text{L}$ ) were recorded with a drop shape analysis system DSA10 Mk2 (KRÜSS Inc.) equipped with a video camera. XPS measurements were carried out on a XPS-APEX (ULVAC PHI Co., Ltd.) using a monochromatic Al- $K_{\alpha}$  X-ray source at takeoff angles of  $45^\circ$ .

Neutron reflectivity (NR) measurements were performed on an ARISA reflectometer using white neutrons with wavelengths of 0.12–0.16 nm at the KENS pulsed-neutron source.<sup>40</sup> As shown in Fig. 1, the neutron beam was irradiated from quartz glass to the interface between  $\text{D}_2\text{O}$  and the immobilized poly(MPC) brush. Incident angles were fixed at 0.3 and  $0.6^\circ$  which covered a  $q$  range of  $0.11\text{--}0.55 \text{ nm}^{-1}$  and  $0.2\text{--}1.1 \text{ nm}^{-1}$ , respectively. The incident slits (S1 and S2) were adjusted to

keep a 55 mm footprint size on the sample surface as well as the angular resolution,  $\Delta\theta/\theta$ , at 5%. The NR profiles were analyzed by fitting calculated reflectivities from model scattering length density profiles to the data, using Parratt32 software.<sup>41</sup>

The friction test was performed on a Tribostation Type32 (Shinto Scientific Co. Ltd.) by sliding a glass ball ( $\phi$  10 mm) on the substrates along a distance of 20 mm at a sliding velocity of  $90 \text{ mm min}^{-1}$  at 298 K. The friction forces of the polymer brushes were measured by a strain gauge and recorded with a PC. The normal load was controlled by placing dead weights (0.49 N) on top of the glass ball holder. The friction coefficient was determined by dividing the friction force by the applied normal load. For each friction measurement, the friction forces of different fresh tracks (10–15) were collected to calculate the friction coefficients and their deviation. A scheme of the friction tester setup was described in a previous paper.<sup>14</sup> Humidity was controlled by blowing a ratio of dry  $\text{N}_2$  gas and humid air. The theoretical contact area between a glass ball probe and a silicon wafer under these conditions can be calculated to be  $3.51 \times 10^{-9} \text{ m}^2$  by Hertz's contact theory, and the average pressure on the contact area was estimated to be 139 MPa.

## Results and discussion

### Hydrophilicity of poly(MPC) brush surface

Controlled polymerization conditions of MPC have been carefully studied by Armes *et al.*,<sup>42</sup> who found out that ATRP of MPC in an alcohol medium proceeds in a living manner even at  $20^\circ\text{C}$  to give a polymer with predicted  $M_n$  and relatively narrow MWD. Various types of water-soluble block copolymers have also been prepared by the ATRP system.<sup>43</sup> RAFT radical polymerization of MPC in water at  $70^\circ\text{C}$  also affords a well-defined polymer.<sup>44</sup> Preparation of high-density well-controlled poly(MPC) brushes has already been reported by Iwasaki *et al.*<sup>18</sup> and Brash *et al.*<sup>45</sup> using surface-initiated ATRP in methanol from a silicon substrate, which was immobilized with an  $\alpha$ -bromoisobutylate moiety by the dipping method. In this study, the authors employed similar polymerization conditions except for the preparation of ATRP initiator monolayers on silicon wafers. AFM analysis revealed that CVA of BHE afforded a quite smooth monolayer surface with no aggregates and low number of defects. XPS spectra of initiator-immobilized silicon wafer showed a carbon signal ( $\text{C}_{1s}$ ) at 286 eV and a bromide ( $\text{Br}_{3d}$ ) signal at 71 eV. The  $\text{C}_{1s}$  signals attributed to C=O and C–O bonds were also observed

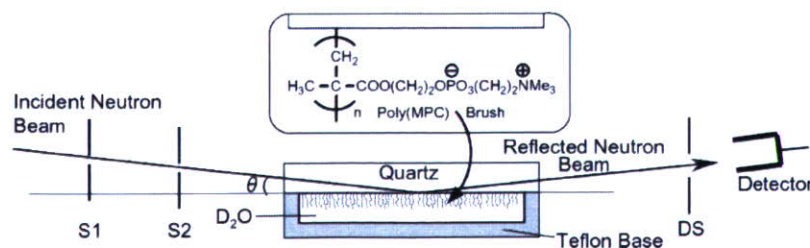


Fig. 1 Schematic view of the solid/liquid cell used in the NR experiments.

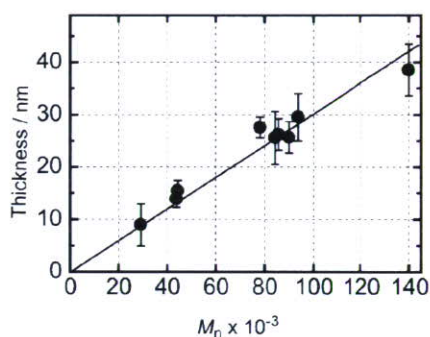


Fig. 2 Relationship between poly(MPC) brush thickness and  $M_n$  of free polymer.

in the narrow scan mode. These results are indicative of formation of a BHE thin layer on the silicon wafer.

Surface-initiated ATRP of MPC was carried out from the BHE-immobilized silicon wafer in the presence of EB as a free initiator coupled with CuBr and 4,4'-dimethyl-2,2'-bipyridyl in methanol. The  $M_n$  of the obtained poly(MPC) brushes on the silicon wafer were estimated to be approximately 30 000–120 000 by SEC of the corresponding free polymer using water as the eluent. The AFM observations revealed that a homogeneous polymer layer was formed on the substrate, and the surface roughness was 0.8–1.5 nm in a dry state in a  $5 \times 5 \mu\text{m}^2$  scanning area. The thickness of the polymer brush was determined to be ca. 10–40 nm by ellipsometry. The graft density was estimated to be ca.  $0.22 \text{ chain nm}^{-2}$  based on the linear relationship between  $M_n$  and the thickness as shown in Fig. 2. The contact angle of water droplets (2.0  $\mu\text{L}$ ) on the poly(MPC) brush surface was very low (Fig. 3(a)). The contact angles against methylene iodide and hexadecane were  $45^\circ$  and  $<5^\circ$ , respectively. Using Owens and Wendt's equation,<sup>46</sup> the surface free energy of the poly(MPC) brush surface was estimated to be  $73 \text{ mN m}^{-1}$ , which is quite similar to that of water. Advancing and receding contact angles of the poly(MPC) brush against water were  $11^\circ$  and  $5\text{--}7^\circ$ , respectively. Fig. 3(b) shows a sphere shaped air bubble (10  $\mu\text{L}$ ) contacting on the brush surface in water.<sup>47</sup> An air bubble easily slips away from the surface by a slight tilting, indicating that the poly(MPC) brush disfavors the contacting with an air and keeps a super-hydrophilic surface.

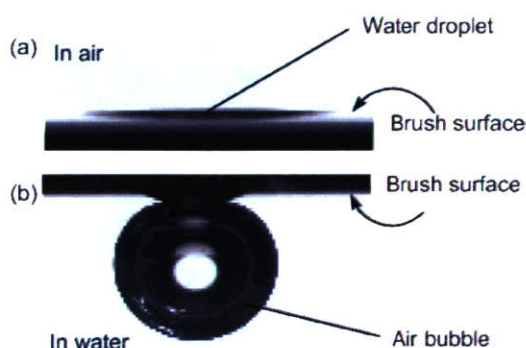


Fig. 3 Contact angle measurements of poly(MPC) brush surface using a water droplet in air (a) and a captured air bubble in water (b).

The behavior of polymer brushes in solvents has important technological implications for various applications. Polymer brushes in good solvents are predicted to adopt a fairly extended conformation due to the high osmotic pressure caused by high local density of polymer chains. However, it is indeed difficult to measure the thickness of the extended brush because a continuous layer of solvated chains will be formed. NR measurements are, therefore, appropriate for the study of the influence of solvent on polymer brush structure. The sample for NR measurements was prepared by surface-initiated ATRP from BHE-immobilized quartz to give a poly(MPC) brush, of which  $M_n$  and polydispersity index ( $M_w/M_n$ ) were 59 500 and 1.5, respectively. A critical  $q$  for the total reflection was clearly observed at  $q = 0.11 \text{ nm}^{-1}$  in Fig. 4 owing to the difference in scattering length density between quartz glass ( $3.80 \times 10^{-4} \text{ nm}^{-2}$ ) and  $\text{D}_2\text{O}$  ( $6.4 \times 10^{-4} \text{ nm}^{-2}$ ). The reflectivity profile arising from the polymer brush interface (Fig. 4(b)) shifted downward compared with that from bare quartz (Fig. 4(a)). This result indicated that the poly(MPC) chains were stretched up to 60–70 nm, and formed a concentration gradient of  $\text{D}_2\text{O}$  in the swelling state. The full length of the graft chain in the all-*trans* conformation is calculated to be 50 nm, assuming the length per monomer unit as 0.25 nm and 200 repeating units. The observed thickness by NR is an acceptable value, since the polymer brush has a distribution in chain length corresponding to the molecular weight distribution ( $M_w/M_n = 1.5$ ).<sup>48</sup> Therefore, the tethered polymer chains would have a fairly extended conformation along the direction normal to the quartz surface. On the other hand, the thickness of the poly(MPC) brush decreased to 30–40 nm in deuterated ethanol- $\text{D}_2\text{O}$  (68 : 32, v/v), as shown

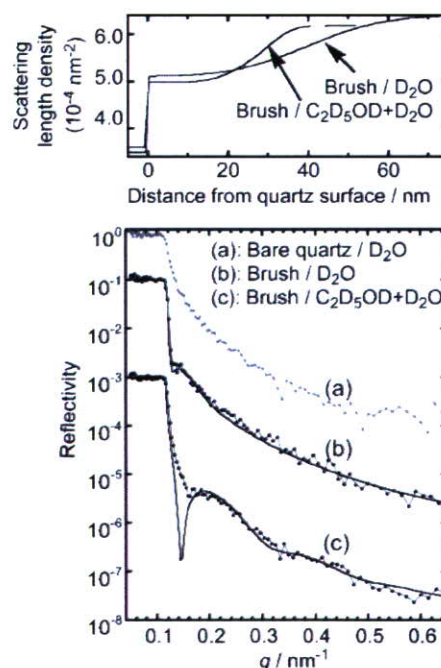


Fig. 4 Experimental NR profiles of bare quartz (a), poly(MPC) brush in  $\text{D}_2\text{O}$  (b), poly(MPC) brush in a mixture of deuterated ethanol- $\text{D}_2\text{O}$  (68 : 32, v/v) (c), and their corresponding fits. Assumed scattering length density profiles for (b) and (c) are shown above.

in Fig. 4(c). Ishihara and Kiritoshi already reported that poly(MPC) was soluble in pure water and pure ethanol, while it was insoluble in a water–ethanol mixture, containing 70–90% of ethanol.<sup>49</sup> Hence the polymer brush is expected to shrink in a poor solvent such as a mixture of deuterated ethanol and D<sub>2</sub>O.

### Frictional properties of poly(MPC) brush surface

The authors previously reported that the friction coefficient of high-density PMMA brushes decreased in response to soaking in toluene whereas they increased in response to immersion in hexane.<sup>14</sup> As toluene is a good solvent for PMMA, the interaction between the brush surface and the sliding probe was moderated, resulting in a surface with low magnitude of friction. Similar behavior was observed in the case of a hydrophilic poly(2,3-dihydroxypropyl methacrylate) brush.<sup>15</sup> These results suggested that the frictional properties largely depend on the solvent quality and the affinity between the brush and probe. In the case of poly(MPC), water plays a role as a good solvent resulting in low friction. Ho *et al.* prepared a low friction surface on polyurethane catheter material by coating with poly(MPC) copolymer.<sup>20</sup> They suggested that the water molecules bound on the surface of poly(MPC) due to hydration provide effective and enhanced boundary lubrication.

Fig. 5(a) shows friction coefficients of poly(MPC) brush surfaces measured by sliding a glass ball in air, water, and toluene at 298 K. Under the dry N<sub>2</sub> gas condition, a high friction coefficient was observed probably due to the strong adhesive interaction between the poly(MPC) brush and the glass probe. In contrast, the brush surface afforded a lower friction coefficient with increasing humidity. It is supposed that water molecules adsorbed onto the surface of the highly hydrophilic poly(MPC) brush, and worked as a lubricant to reduce the interaction between brush and probe. In addition, water-swollen poly(MPC) brushes compressed by a probe glass ball would give a repulsive force against a high normal load due to the osmotic pressure originating from steric repulsion of the high-density brushes.<sup>50</sup> These water-lubrication systems restricted the direct contact of a probe with the substrate to

reduce the friction force. Contrary to our expectation, the friction coefficient in water was higher than that in humid air conditions. The authors suppose that swollen and extended poly(MPC) brush chains in water should have larger actual contact area between brush and probe to result in higher friction coefficient, compared with in the case of humid air. In toluene, which is poor solvent for poly(MPC), a higher friction coefficient was observed, probably because hydrophilic poly(MPC) would be unwilling to be in contact with a poor solvent, and prefer to interact with the hydrophilic glass ball surface, thus giving a higher friction coefficient.

A similar lubrication tendency was observed when a brush-immobilized glass ball was used as a sliding probe, as shown in Fig. 5(b). The friction coefficient under the highly humidified air condition was significantly reduced to 0.02, which is lower than that in aqueous conditions. It is supposed that hydrophilic MPC units covered with water molecules effectively reduced the friction force, creating a good water lubrication system. Basically, a mutual interpenetration of brushes in water supposed to be limited by excluded volume effects of dense grafting chains. However, the polymer brush had a distribution in chain length as mentioned above; the density of chains at the outer surface of the brush must be lower than that at the inside of the brush layer. Interdigitation of brush chains can occur in the limited outer surface of the brush layer, in particular, at the thin layer of the brush–brush interface in water. Fairly extended poly(MPC) chains in water are expected to have a larger interdigitation region than the swollen brush in humidified air conditions. This is a reason why, the authors suppose, poly(MPC) brushes in water showed a higher friction coefficient than in humid air conditions. Additionally, an unexpected phenomenon was observed in toluene. The friction coefficient in toluene was slightly lower than that in water, even though an adhesive interaction between brush and brush in toluene must be stronger than that in a good solvent. This is the opposite result compared with Fig. 5(a). In a poor solvent, a mutual interpenetration of brushes is rather hard to occur compared with in a good solvent because the mutual brush chains should be shrinking in a poor solvent. Therefore, the authors supposed that water molecules adsorbed on the surface of hydrophilic poly(MPC) brush formed a thin

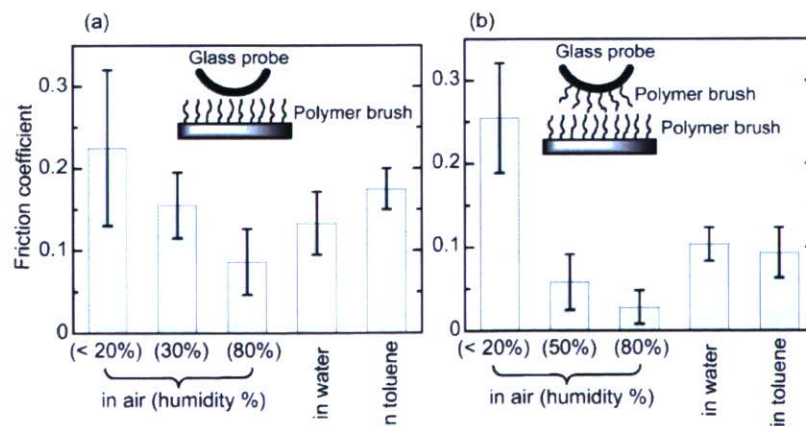


**Fig. 5** Friction coefficient of poly(MPC) brush in air, water and toluene solution by sliding a glass ball over a width of 20 mm at a sliding velocity of 90 mm min<sup>-1</sup> under loading of 0.49 N at 298 K.

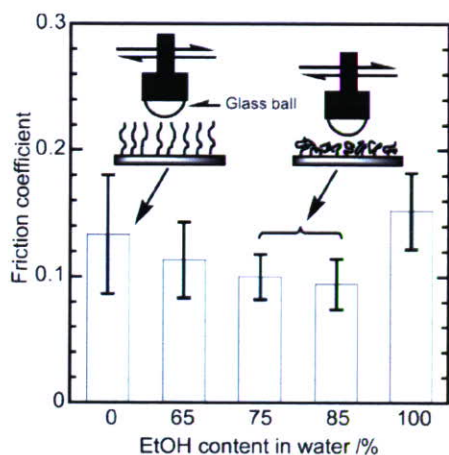


**Fig. 6** Friction coefficient of poly(MPC) brushes in ethanol-water solutions by sliding a glass ball over a width of 20 mm at a sliding velocity of  $90 \text{ mm min}^{-1}$  under loading of  $0.49 \text{ N}$  at  $298 \text{ K}$ .

boundary layer between the brush-brush interface under the poor solvent and humid air conditions, giving a fluid lubrication and a low friction. On the other hand, interdigitation of brushes in a good solvent, such as water, would afford a continuous layer between brush on substrate and brush on probe interfaces to give a larger friction resistance, although additional experimental evidence is needed to confirm this hypothesis. Klein and his co-workers pointed out that highly compressed polymer brush layers between the surfaces behaved in a solid-like manner.<sup>51</sup> For the further discussion on the frictional mechanism of poly(MPC) brushes, the viscoelastic properties of brushes, the effect of squeezed hydrodynamic lubrication,<sup>52</sup> and adhesive force measurements of brush surfaces would also be required.

Fig. 6 shows the frictional properties of poly(MPC) brushes in ethanol-water mixtures. The friction coefficient decreased with ethanol content in water ranging from 65 to 85%, and increased again in pure ethanol (100%). Even though an 85% ethanol solution in water is a poor solvent for poly(MPC) as mentioned above, a lower friction coefficient was observed than in a good solvent such as pure ethanol. Interestingly, these are contradictory results which are mentioned in Fig. 5(a) and the previous reports.<sup>14,15</sup> NR measurements revealed that the structure and the thickness of poly(MPC) brushes at the aqueous interface were sensitive to the content of ethanol in the water mixture. The authors supposed that swollen and

extended poly(MPC) brush chains in a good solvent should have increased actual contact area between brush and glass probe, because of a large decrease in apparent modulus. A large contact region in a good solvent might result in a higher friction coefficient, compared with the shrinking brush in a poor solvent. Toluene and 85% ethanol aqueous solution are both poor solvents for poly(MPC), however, the interaction between the super-hydrophilic poly(MPC) brush and the hydrophilic glass probe in hydrophobic toluene solution would be stronger than that in 85% ethanol aqueous solution because water molecules adsorb on poly(MPC) and the glass probe to reduce the adhesive force between their surfaces.

The wear resistance of poly(MPC) brushes in humid air was also investigated. A cast film was prepared by spin casting from a methanol solution of poly(MPC) as a control. Fig. 7(a) shows the time dependence of the friction coefficient of cast film and sliding by a glass ball under a normal load of  $0.098 \text{ N}$  in air (humidity = 50%). The friction coefficient of the cast film began to increase within the early stage of the friction test, and attained a magnitude of 0.2 within 400 sec. This result indicates that the surface polymer is easily scratched away by a sliding glass probe. In air conditions over 75% humidity, a cast film adsorbs moisture from air to become a swollen layer, which is readily swept out from the silicon wafer by the sliding probe. Fig. 7(b) shows a friction test of a poly(MPC) brush surface under a load of  $0.49 \text{ N}$  in humid air (humidity > 75%). A low friction coefficient of the poly(MPC) brush was continuously observed in spite of the higher normal load, implying good wear resistance. Actually, the friction coefficients slightly increased with sliding time, however, they were still around 0.1 even after 1600 sec. Wear resistance was improved due to the anchoring effect of the tethered polymer chain end by covalent bonds on the substrate.

## Conclusion

In conclusion, the authors prepared dense poly(MPC) brushes on silicon wafers by surface-initiated ATRP, resulting in super-hydrophilic surfaces. Macroscopic frictional properties of the poly(MPC) brush surface largely depended on the humidity and solvent quality. The extremely low friction coefficient was observed in an aqueous medium with sliding by brush-bearing surfaces. The authors suppose that osmotic repulsions arising from high-density grafting chains in water afford weak interpenetration between the opposing and compressed brushes even at a large normal load, resulting in a low friction

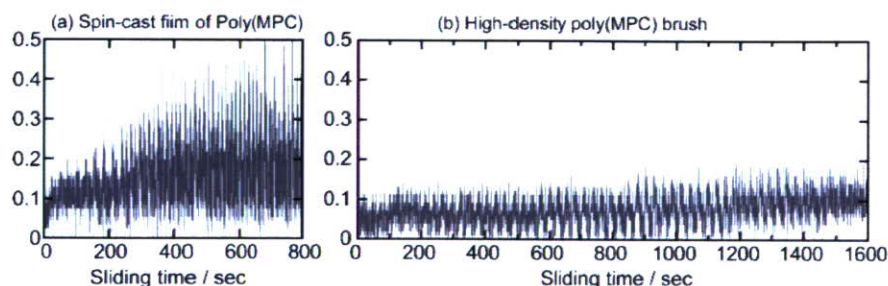


**Fig. 7** Friction time dependence of friction coefficient on cast film of poly(MPC) (a) and poly(MPC) brush (b) at a sliding velocity of  $90 \text{ mm min}^{-1}$  in air:  $M_n$  of poly(MPC) = 80 800. (a) Humidity = 50%, normal load =  $0.098 \text{ N}$ . (b) Humidity > 75%, normal load =  $0.49 \text{ N}$ .

surface. This study showed that boundary lubrication was achieved through the super-hydrophilic poly(MPC) brush even in humid air by significantly decreasing the friction coefficient of the surface. Experiments to explore the relation between adhesion and lateral lubrication forces between brush surfaces are currently in progress.

## Acknowledgements

This research was supported by a Grant-in-Aid for "Joint Project of Chemical Synthesis Core Research Institutions" from the Ministry of Education, Culture, Science, Sports and Technology of Japan. N. H. appreciates the Research Fellowships of the Japan Society for the Promotion of Science for Young Scientists.

## References

- L. Lapcik, Jr., L. Lapcik, S. De Smedt, J. Demeester and P. Chabreck, *Chem. Rev.*, 1998, **98**, 2663–2684.
- I. F. Radaeva, G. A. Kostina and A. V. Zmievskii, *Appl. Biochem. Microbiol.*, 1997, **33**, 111–115.
- J. Rühle, in *Polymer Brushes*, ed. R. C. Advincula, W. J. Brittain, K. C. Caster and J. Rühle, Wiley-VCH, Weinheim, 2004, pp. 1–31.
- J. Klein, E. Kumacheva, D. Mahalu, D. Perahia and L. J. Fetters, *Nature*, 1994, **370**, 634–636.
- N. Kampf, J.-F. Gohy, R. Jerome and J. Klein, *J. Polym. Sci. Part B: Polym. Phys.*, 2005, **43**, 193–204.
- U. Raviv, S. Giasson, N. Kamph, J. F. Gohy, R. Jérôme and J. Klein, *Nature*, 2003, **425**, 163–165.
- Y. Ohsedo, R. Takashina, J. P. Gong and Y. Osada, *Langmuir*, 2004, **20**, 6549–6555.
- S. R. Sheth, N. Efremova and D. E. Leckband, *J. Phys. Chem. B*, 2000, **104**, 7652–7662.
- S. Lee, M. Müller, M. Ratoi-Salagean, J. Vörös, S. Pasche, S. M. De Paul, H. A. Spikes, M. Textor and N. D. Spencer, *Tribol. Lett.*, 2003, **15**, 231–239.
- M. Müller, S. Lee, H. A. Spikes and N. D. Spencer, *Tribol. Lett.*, 2003, **15**, 395–405.
- Y. Tsujii, K. Ohno, S. Yamamoto, A. Goto and T. Fukuda, *Adv. Polym. Sci.*, 2006, **197**, 1–45.
- S. Yamamoto, M. Ejaz, Y. Tsujii and T. Fukuda, *Macromolecules*, 2000, **33**, 5602–5608.
- Y. Tsujii, K. Okayasu, K. Ohno and T. Fukuda, *Polym. Prepr. (Am. Chem. Soc., Div. Polym. Chem.)*, 2005, **230**, U4189.
- Y. Sakata, M. Kobayashi, H. Otsuka and A. Takahara, *Polym. J.*, 2005, **37**, 767–775.
- M. Kobayashi and A. Takahara, *Chem. Lett.*, 2005, **34**, 1582–1583.
- K. Ishihara, T. Ueda and N. Nakabayashi, *Polym. J.*, 1990, **22**, 355–360.
- K. Ishihara, H. Nomura, T. Mihara, K. Kurita, Y. Iwasaki and N. Nakabayashi, *J. Biomed. Mater. Res.*, 1998, **39**, 323–330.
- R. Iwata, P. Suk-In, V. P. Hoven, A. Takahara, K. Akiyoshi and Y. Iwasaki, *Biomacromolecules*, 2004, **5**, 2308–2314.
- W. Feng, S. Zhu, K. Ishihara and J. L. Brash, *Biointerphases*, 2006, **1**, 50–60.
- S. P. Ho, N. Nakabayashi, Y. Iwasaki, T. Boland and M. LaBerge, *Biomaterials*, 2003, **24**, 5121–5129.
- T. Moro, Y. Takatori, K. Ishihara, T. Konno, Y. Takigawa, T. Matsushita, U. Chung, K. Nakamura and H. Kawaguchi, *Nat. Mater.*, 2004, **3**, 829–836.
- J. Ruhe, M. Ballauff, M. Biesalski, P. Diczok, F. Gröhn, D. Johannsmann, N. Houbenov, N. Hugenberg, R. Konradi, S. Minko, M. Motornov, R. R. Netz, M. Schmidt, C. Seidel, M. Stamm, T. Stephan, D. Usov and H. Zhang, *Polyelectrolyte Brushes*, in *Adv. Polym. Sci., Polyelectrolytes with Defined Molecular Architecture I*, ed. M. Schmidt, Springer, New-York, 2004, vol. **165**, pp. 79–150.
- I. Luzinov, S. Minko and V. V. Tsukruk, *Prog. Polym. Sci.*, 2004, **29**, 635.
- S. J. Miklavic and S. Marčelja, *J. Phys. Chem.*, 1988, **92**, 6718–6722.
- R. Israels, F. A. M. Leermakers, G. J. Fleer and E. B. Zhulina, *Macromolecules*, 1994, **27**, 3249–3261.
- Y. V. Lyatskaya, F. A. M. Leermakers, G. J. Fleer, E. B. Zhulina and T. M. Birshtein, *Macromolecules*, 1995, **28**, 3562–3569.
- E. B. Zhulina, J. K. Wolterink and O. V. Borisov, *Macromolecules*, 2000, **33**, 4945–4953.
- P. Pincus, *Macromolecules*, 1991, **24**, 2912–2919.
- R. S. Ross and P. Pincus, *Macromolecules*, 1992, **25**, 2177–2183.
- V. A. Pryamitsyn, F. A. M. Leermakers, G. J. Fleer and E. B. Zhulina, *Macromolecules*, 1996, **29**, 8260–8270.
- H. J. Taunton, C. Toprakcioglu, L. J. Fetters and J. Klein, *Nature*, 1988, **332**, 712–714.
- E. Eiser, J. Klein, T. A. Witten and L. J. Fetters, *Phys. Rev. Lett.*, 1999, **82**, 5076–5079.
- S. Minko, *J. Macromol. Sci., Polym. Rev.*, 2006, **46**, 397–420.
- T. McPherson, A. Kidane, I. Szeleifer and K. Park, *Langmuir*, 1998, **14**, 176–186.
- S. Hayashi, T. Abe, N. Higashi, M. Niwa and K. Kurihara, *Langmuir*, 2002, **18**, 3932–3944.
- T. W. Kelley, P. A. Shorr, D. J. Kristin, M. Tirrell and C. D. Frisbie, *Macromolecules*, 1998, **31**, 4297–4300.
- K. Ohno, T. Morinaga, K. Koh, Y. Tsujii and T. Fukuda, *Macromolecules*, 2005, **38**, 2137–2142.
- M. Husseman, E. E. Malmstrom, M. McNamara, M. Mate, D. Mecerreyes, D. G. Benoit, J. L. Hedrick, P. Mansky, E. Huang, T. P. Russell and C. J. Hawker, *Macromolecules*, 1999, **32**, 1424–1431.
- K. Hayashi, N. Saito, H. Sugimura, O. Takai and N. Nagagiri, *Langmuir*, 2002, **18**, 7469–7472.
- N. Torikai, M. Furusaka, H. Matsuoka, Y. Matsushita, M. Shibayama, A. Takahara, M. Takeda, S. Tasaki and H. Yamaoka, *Appl. Phys. A: Mater. Sci. Process.*, 2002, **74**, S264–266.
- C. Braun, *Parratt 32 software*, Berlin Neutron Scattering Center (BENS), Hahn-Meitner Institut, Berlin, 1997.
- Y. Ma, E. J. Lobb, N. C. Billingham, S. P. Armes, A. L. Lewis, A. W. Lloyd and J. Salvage, *Macromolecules*, 2002, **35**, 9306–9314.
- Y. Ma, Y. Tang, N. C. Billingham, S. P. Armes, A. L. Lewis, A. W. Lloyd and J. Salvage, *Macromolecules*, 2003, **36**, 3475–3484.
- S. Yusa, K. Fukuda, T. Yamamoto, K. Ishihara and Y. Morishima, *Biomacromolecules*, 2005, **6**, 663–670.
- W. Feng, S. Zhu, K. Ishihara and J. L. Brash, *Langmuir*, 2005, **21**, 5980–5987.
- D. K. Owens and R. C. Wendt, *J. Appl. Polym. Sci.*, 1969, **13**, 1741–1747.
- W. C. Hamilton, *J. Colloid Interface Sci.*, 1972, **40**, 219–222.
- S. T. Milner, T. A. Witten and M. F. Cates, *Macromolecules*, 1989, **22**, 853–861.
- Y. Kiritoshi and K. Ishihara, *J. Biomater. Sci., Polym. Ed.*, 2002, **13**, 214–224.
- S. Yamamoto, M. Ejaz, Y. Tsujii, M. Matsumoto and T. Fukuda, *Macromolecules*, 2000, **33**, 5608–5612.
- J. Klein, Y. Kamiyama, H. Yoshizawa, J. N. Israelachvili, G. H. Fredrickson, P. Pincus and L. J. Fetters, *Macromolecules*, 1993, **26**, 5552–5560.
- G. H. Fredrickson and P. Pincus, *Langmuir*, 1991, **7**, 786–795.



## Nanoscale Surface Grafting with Phospholipid Polymer to Lubricate Polypropylene Surface

Kazuhiko Kitano<sup>1</sup>, Ryosuke Matsuno<sup>2,3</sup>, Tomohiro Konno<sup>2,3</sup>,  
Madoka Takai<sup>2,3</sup>, and Kazuhiko Ishihara<sup>1,2,3</sup>

<sup>1</sup>Department of Bioengineering, <sup>2</sup>Department of Materials Engineering, School of Engineering, <sup>3</sup>Center for NanoBio Integration, The University of Tokyo, 7-3-1, Hongo, Bunkyo-ku, Tokyo 113-8656, Japan, Fax: +81-3-5841-8647, e-mail: kitano@mpc.t.u-tokyo.ac.jp

The purpose of this study is obtaining both biocompatibility and lubricity to biomaterial surfaces. For this purpose, we investigated the effects of a graft polymerization of 2-methacryloyloxyethyl phosphorylcholine (MPC) onto polypropylene (PP) surface. The MPC graft nanolayer was prepared using a photo-induced graft polymerization. The poly(MPC)-grafted (PMPC-g-PP) surface was characterized by X-ray photoelectron spectroscopy (XPS), attenuated total reflection Fourier transform infrared spectroscopy (ATR-FTIR), and static and dynamic water contact angle measurements. As a result, the PMPC grafting clearly increased hydrophilicity and surface mobility. Friction coefficient was measured in air and in water. The friction coefficient of the PMPC surface was 0.019 in water, which was 1/10 compared with air condition. This value is similar to that of the human joints. After the friction test in water, the surface was observed with scanning electron spectroscopy. No flaw was observed on the PMPC surface. It was considered that the PMPC surface showed the behavior of hydrodynamic lubrication in water. Friction test was also performed under biological conditions; in phosphate buffered saline (PBS), PBS containing a bovine serum albumin, and cell culture medium containing fetal bovine serum. The results indicated that the PMPC surface kept highly lubricity under biological conditions.

Key words: phospholipid polymer, photo-induced graft polymerization, friction, hydrodynamic lubrication

### 1. INTRODUCTION

In recent years there has been increasing interest in surface modification with polymers to give a solid surface necessary surface properties. Among many surface properties, we aimed for giving both biocompatibility and lubricity to biomaterial surface. Lubricity is one of the essential properties for biomaterials such as artificial joints, blood pump bearings, and catheters. As for artificial joints, the loosening caused by wear between the articulating surfaces is the most serious problem limiting their survival and clinical success.

Surface modification is conducted using a variety of methods such as a plasma treatment, physical coating, and surface grafting. In this study we choose a surface-initiated photo-induced graft polymerization method. This polymerization has advantages in simplicity, efficiency and general versatility. The grafting location can be restricted to the surface attached benzophenone used as a photoinitiator. Using this method, we can obtain a polymer-grafted surface with strongly tethering by a covalent bond.

Selection of the grafting polymer is the next parameter. We used 2-methacryloyloxyethyl phosphorylcholine (MPC), which is well known for biocompatible polymer whose side chain is composed of phosphorylcholine resembling phospholipid of cell membrane<sup>1-4</sup>. The polymers with MPC units onto the surface of medical devices have already been shown to suppress biological reactions when they are in contact with living organisms. By using the fundamental

research results, the MPC polymers are now clinically used on the surfaces of intravascular stents, guide wires, soft contact lenses, and artificial lung<sup>5-7</sup>. Surface grafting of the MPC polymer is also excellent method to obtain the biocompatibility<sup>8-10</sup>. We expected that the MPC polymer grafting improve not only biocompatibility but also lubricity of a solid surface because there are the same phosphorylcholine groups on the surface of the human articular cartilage. It has been reported that the MPC polymer grafting onto the polyethylene liner of the artificial hip joint clearly reduced wear between the articulating surfaces for long term<sup>11</sup>. But why the MPC polymer grafting increases surface lubricity has not been clear yet. In this study we investigated the mechanism of lubricity of MPC polymer grafted surface. We studied the mechanical and biological effects of the MPC grafting onto the surface of polypropylene (PP).

### 2. EXPERIMENTS

#### 2.1 Preparation of poly(MPC)-grafted PP (PMPC-g-PP) surface

The grafting of MPC on PP surface was carried out by photo-induced graft polymerization<sup>12</sup>. The PP substrates were cut into 2.5cm x 7.5cm x 0.1cm(t) and rinsed sufficiently with acetone and hexane. The substrates were immersed in an acetone solution containing 0.5wt% benzophenone for 1min. The substrates were dried in vacuo under dark condition overnight at room temperature. The 0.5mol/L of MPC aqueous solution was prepared in degassed pure water. The benzophenone coated PP substrates were immersed in the MPC

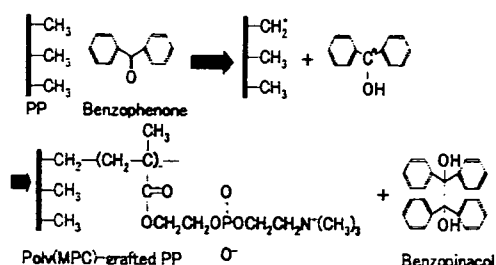


Fig.1 Synthesis route of the PMPC-g-PP surface

monomer solution. The photo polymerization on the PP surface was carried out using a 500W ultra-high pressure mercury lamp for 120 min at 60°C. After the reaction, the substrates were successively washed in water and ethanol and dried in vacuo for 24h at room temperature. The scheme of the reaction is shown in Fig.1.

## 2.2 Surface characterization

**XPS:** The surface chemical composition was determined by X-ray photoelectron spectroscopy (XPS). All samples were completely dried in vacuo before use. Survey scans (0-1100eV) were performed to identify the C, N, O, and P elements. A take off angle of the photoelectrons was 90°. All binding energies were referenced the  $\text{C}_{1s}$  peak at 285.0eV.

**ATR-FTIR:** The measurement of the IR spectrum of the surface modified and unmodified PP substrates was carried out with an attenuated total reflection (ATR) apparatus spectrometer under dry conditions. The spectra were recorded from  $650\text{ cm}^{-1}$  to  $4000\text{ cm}^{-1}$  at a  $4\text{ cm}^{-1}$  resolution. A single beam reference spectrum of a freshly cleaned ZnSe crystal at an incident angle of  $45^\circ$  was recorded before the measurements and used as the background spectrum.

**Water contact angle:** The static water contact angles were measured using a goniometer at room temperature. The samples were dried in vacuo for 24h before the measurements. Water droplets of 6 $\mu\text{L}$  were contacted onto the substrates and the contact angles at 10s were directly measured by photographic images. The data was collected at 5 positions on each sample. The advancing and receding contact angle were measured using Wilhelmy plate method. The data was averaged through 4 cycles.

## 2.3 Friction test

The surface kinetic frictional coefficients were measured using a tribo-tester. The schematic illustration of the tribo-tester is shown in Fig.2. The samples were dried in vacuo for 24h before the measurements. The measurements were carried out in air, in water, and under biological conditions: in phosphate buffered saline (PBS), PBS solution containing 0.45g/dL of a bovine serum albumin (albumin-PBS), and cell culture medium containing 10% fetal bovine serum (FBS). The measurements were conducted by sliding the substrates under a 50g load using a stainless-steel ball (10mm in diameter). The sliding speed was 10mm/sec and the sliding scale was 20mm. The sliding repeated 100 cycles.

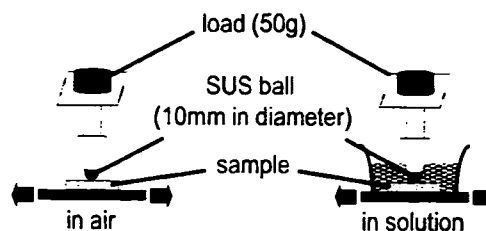


Fig.2 Schematic illustration of the tribo-tester. The left side is the friction test in air, and the right side is in solutions. Load was 50g, the jig was a stainless-steel ball (10mm in diameter), the sliding speed was 10mm/sec, and the sliding scale was 20mm.

After the friction test in water, the surfaces were observed with Scanning electronic microscopy (SEM).

## 3. RESULTS AND DISCUSSIONS

### 3.1 MPC graft polymerization on PP

Fig.1 illustrates the MPC graft polymerization scheme on the PP surface. The benzophenone absorbed on the substrate exhibits a well-known photochemical reaction. The benzophenone is excited to the triplet state, which extracts a hydrogen atom from the  $\alpha$ -methyl group of the substrate to produce polymer radicals capable of initiating graft polymerization of the monomers. The excited benzophenone finally changes to benzopinacol. The location of MPC polymerization was restricted to the surface because radicals as the starting points of the polymerization were only produced on the surface and MPC was not dissolved in PP.

### 3.2 Surface characterization

The stable grafting of MPC on the PP was confirmed using XPS (Fig.3). The peaks in the carbon atom region ( $\text{C}_{1s}$ ) at 286.5eV and 289eV indicated the ether bond and the ester bond, respectively, and those in the nitrogen atom region ( $\text{N}_{1s}$ ) at 403eV and phosphorus atom region ( $\text{P}_{2p}$ ) at 133eV were specific to the phosphorylcholine group in the MPC unit.

Fig.4 shows the ATR-FTIR spectra of the PP and the PMPC-g-PP surface under dry conditions. Among the PMPC-g-PP surface, the peak at  $1719\text{ cm}^{-1}$  corresponded to the ester group in the MPC and a few peaks between  $800\text{ cm}^{-1}$  and  $1300\text{ cm}^{-1}$  originated from the phosphorylcholine group in the MPC unit.

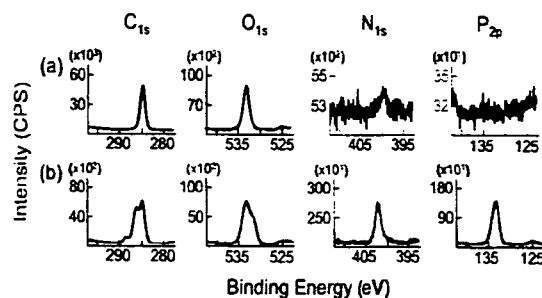


Fig.3 XPS charts of (a) unmodified PP and (b) PMPC-g-PP surface

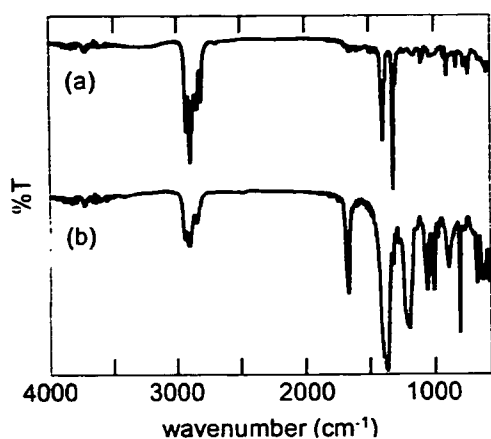


Fig.4 ATR-FTIR spectrum of (a) unmodified PP and (b) PMPC-g-PP surface

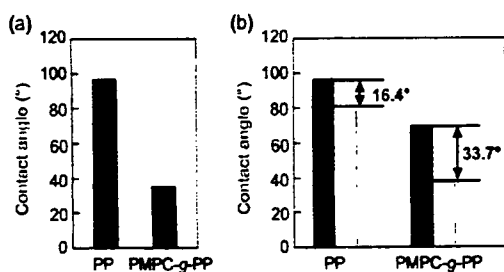


Fig.5 Water contact angle of PP and PMPC-g-PP surface. (a) Static contact angle. (b) dynamic contact angle. black bars: advancing contact angle. white bars: receding contact angle

Fig.5 shows the static and dynamic water contact angle of the PP and the PMPC-g-PP surface. The static contact angle on the PMPC-g-PP surface was  $35.6^\circ$ , which was about 1/3 of those on the unmodified PP surface. This result indicated that the PMPC grafting on PP surface greatly increased hydrophilicity. From the result of hysteresis between the advancing contact angle and the receding contact angle, hysteresis of the PMPC-g-PP surface was about two times larger than that of unmodified PP. This result was caused by extending of PMPC graft chains in water because PMPC had high hydrophilicity. It was confirmed that PMPC-g-PP surface had large surface mobility in water.

### 3.3 Friction properties

Fig.6 shows the kinetic friction coefficients of the PMPC-g-PP surface and unmodified PP at every 10 cycle in air and in water. In air, the friction coefficient of the PMPC-g-PP surface was 0.20, which is the same frictional property as that of unmodified PP. However in water, the lubricity of the PMPC-g-PP surface was greatly increased. The average of the friction coefficient of the PMPC-g-PP surface in water was 0.019, which reduced 90% compared with air condition and reduced 89% compared with unmodified PP in water. This value is similar to that of the human joints. These results

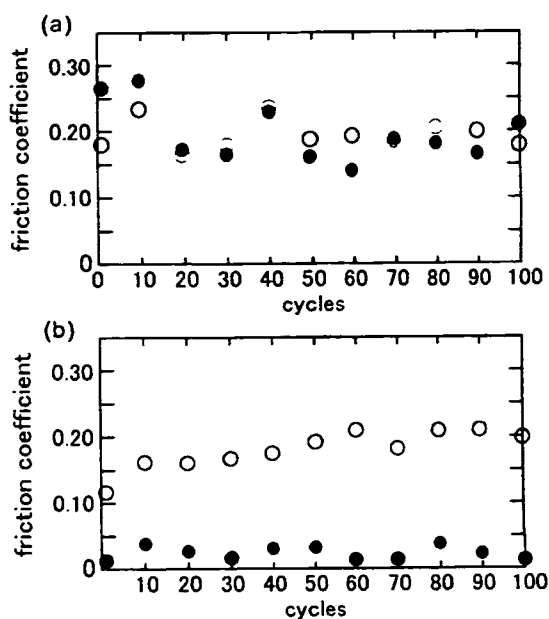


Fig.6 Friction coefficient of PP and PMPC-g-PP surface. The measurement was carried out (a) in air and (b) in water. white circle: unmodified PP. black circle: PMPC-g-PP surface.

indicated that the presence of water is a necessary condition for lubricating the PP surface by PMPC grafting.

Fig.7 shows the SEM observation of the PP and the PMPC-g-PP surface before and after the friction test in water. There was a flaw on the unmodified PP surface made by the friction test, while no flaw was observed on the PMPC-g-PP surface. It was considered that the grafted PMPC could keep hydration layer between the frictional surfaces and this hydrated PMPC layer completely kept the frictional surfaces apart during the friction test. The PMPC-g-PP surface showed the behavior of hydrodynamic lubrication in water.

Our solution of the lubricity mechanism is as follows. On the condition of hydrodynamic lubrication, surface friction is dependent on the mobility of liquid layer between the friction surfaces. Kitano found that the PMPC had a very small effect on the structure of the hydrogen-bonding network of water molecules<sup>13</sup>. The structure of hydrated layer in the vicinity of the PMPC graft chains are similar to that of bulk water which has high mobility. In short, the reason why the PMPC-g-PP surface clearly reduces surface friction in water is that the PMPC graft chains have high mobile hydrated layer between the friction surfaces. In air in which hydrated later could not exist, friction coefficient of PMPC-g-PP had no difference from that of unmodified PP in spite of PMPC existed on the surface.

Friction test was also performed under biological conditions. Fig.8 shows the friction coefficients of the PP and the PMPC-g-PP surface at every 10 cycle in PBS, in albumin-PBS, and in FBS. The average of the friction coefficient of unmodified PP was 0.30 in albumin-PBS and 0.25 in FBS. These values were clearly higher than those in water and in PBS. We expected that protein adsorption onto the unmodified PP surface caused this

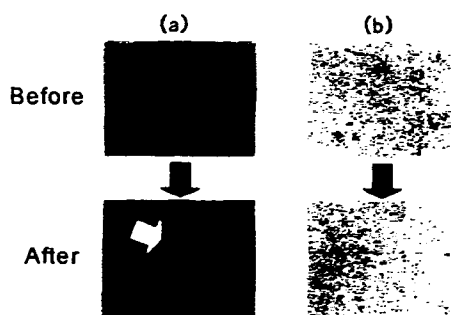


Fig.7 SEM images of (a) unmodified PP and (b) PMPC-g-PP surface before and after the friction test in water through 100 cycles.

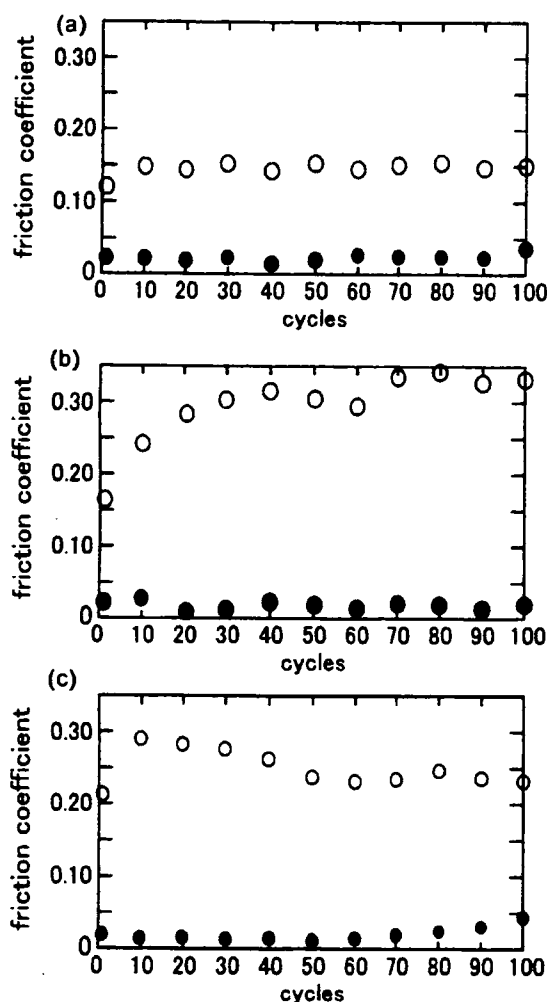


Fig.8 Friction coefficient of PP and PMPC-g-PP surface. The measurement was carried out (a) in PBS, (b) in PBS solution containing 0.45g/dL of a bovine serum albumin, (c) in cell culture medium containing 10% of fetal bovine serum, white circle: unmodified PP, black circle: PMPC-g-PP surface.

high friction coefficient. On the other hand, the friction coefficients of the PMPC-g-PP surface were 0.022 in PBS, 0.017 in albumin-PBS, and 0.017 in FBS. These results were equal to those in water. Lubrication properties of the PMPC-g-PP surface were not affected by every ion or protein. In short, the PMPC grafting could give not only high lubricity but also good biocompatibility.

#### 4. CONCLUSIONS

We reported the preparation of a poly(MPC)-grafted PP in order to enhance its surface hydrophilicity, biocompatibility, and lubricity. A convenient polymerization was conducted using the UV-induced free radical "grafting-from" method based on the physically absorbed benzophenone on the PP. Friction test revealed the reduced friction coefficients on the PMPC-g-PP surface in water. The value of the friction coefficients of the PMPC-g-PP surface was similar to that of human joints. SEM observation indicated that the hydrated layer around the PMPC graft chains kept the frictional surfaces apart. It was concluded that the presence of this nanoscale hydrated layer, which had high mobility like bulk water, leads to the high lubricity. This high lubricity was maintained under the biological conditions. The PMPC grafting on solid surfaces is available for improving frictional properties of many medical devices.

#### 5. REFERENCES

- [1] K. Ishihara, T. Ueda, and N. Nakabayashi, *Polym. J.*, **32**, 355-360 (1990)
- [2] K. Ishihara, N. P. Ziats, B. P. Tierney, N. Nakabayashi, and J. M. Anderson, *J. Bone Miner. Res.*, **25**, 1397-1407 (1991)
- [3] K. Ishihara, H. Oshida, T. Ueda, Y. Endo, A. Watanabe, and N. Nakabayashi, *J. Bone Miner. Res.*, **26**, 1543-1552 (1992)
- [4] P. C. Chang, S. Lee, and G. Hsiue, *J. Bone Miner. Res.*, **39**, 380-389
- [5] S. Kihara, K. Yamazaki, K. N. Litwak, P. Litwak, M. V. Kameneva, H. Ushiyama, T. Tokuno, D. C. Borzelleca, M. Umez, J. Tomioka, O. Tagusari, T. Akimoto, H. Koyanagi, H. Kurosawa, R. L. Kormos, and B. P. Griffith, *Artif. Organs*, **27**, 188-192 (2003)
- [6] A. L. Lweis, *Colloids Surf. B*, **18**, 261-275 (2000)
- [7] A. L. Lweis, L. A. Tolhurst, and P. W. Startford, *Biomaterials*, **23**, 1697-1706 (2002)
- [8] K. Ishihara, N. Nakabayashi, K. Fukumoto, and J. Aoki, *Biomaterials*, **13**, 145-149 (1992)
- [9] R. Iwata, P. Suk-In, V. P. Hoven, A. Takahara, K. Akiyoshi, and Y. Iwasaki, *Biomacromolecules*, **5**, 2308-2314 (2004)
- [10] W. Feng, S. Zhu, K. Ishihara, and J. L. Brash, *Langmuir*, **21**, 5980-5987 (2005)
- [11] T. Moro, Y. Takatori, K. Ishihara, T. Konno, Y. Takigawa, T. Matsushita, U. Chung, K. Nakamura, and H. Kawaguchi, *Nature Materials*, **3**, 829-835 (2004)
- [12] K. Ishihara, Y. Iwasaki, S. Ebihara, Y. Shindo, and N. Nakabayashi, *Colloids Surf. B*, **18**, 325-335 (2000)
- [13] H. Kitano, M. Imai, T. Mori, M. G. Ide, Y. Yokoyama, and K. Ishihara, *Langmuir*, **19**, 10260-10266 (2003)